2012

The Repair of Laterally Damaged Concrete Bridge Girders Using Carbon Fiber Reinforcing Polymers (CFRP)

Matthew Kent Graeff
University of North Florida

THE REPAIR OF LATERALLY DAMAGED CONCRETE BRIDGE GIRDERS USING CARBON FIBER REINFORCING POLYMERS (CFRP)

by

Matthew Kent Graeff

A thesis submitted to the School of Engineering in partial fulfillment of the requirements for the degree of

Master of Science in Civil Engineering

UNIVERSITY OF NORTH FLORIDA

COLLEGE OF COMPUTING, ENGINEERING, & CONSTRUCTION

April, 2012

CERTIFICATE OF APPROVAL PAGE

The thesis "The Repair of Laterally Damaged Concrete Bridge Girders using Carbon Fiber Reinforcing Polymers (CFRP)" submitted by (Matthew K. Graeff)

Approved by the thesis committee: (Date)

Signature Deleted

4/4/12

Dr. N. Michael Jackson

Signature Deleted

Dr. James Fletcher

Signature Deleted

4/4/12

Dr. Adel ElSafty
Committee Chairperson

Accepted for the Department:

Signature Deleted

4/25/12

Dr. Murat Tiryakioglu
Chairperson

Accepted for the College:

Signature Deleted

4/26/12

Dr. Mark A. Tumeo
Dean

Accepted for the University:

Signature Deleted

5/21/12

Dr. Len Roberson
Dean of Graduate Studies

ACKNOWLEDGMENTS

The author would like to thank the Florida Department of Transportation for their support and interest in this research. Also, appreciation is extended to the Fyfe Corporation and Gate Precast Concrete Company for their participation and donations in regards to this research. In particular, special thanks go out to Rodney Chamberlain (the project manager), Sam Fallaha, David Wagner, and William Potter the engineers of the FDOT Structural research center in Tallahassee, Florida. The author would also like to include a special thanks to the laboratory staff at the FDOT Structural Research center including Paul, Steve, Chris, Frank, Tony, Dave, and all of the OPS guys/gals.

On a more personal level the author would like to thank the members of his committee Dr. Adel ElSafty, Dr. Mike Jackson, and Dr. James Fletcher for their guidance throughout the process of the research. Also, thanks to all family and friends for their enduring support.

TABLE OF CONTENTS

LIST OF TABLES

CHAPTER

LIST OF FIGURES

CHAPTER

ABSTRACT

In recent years the use of carbon fiber reinforcing polymers (CFRP) to repair damaged structural components has become more accepted and practiced. However, the current reference for designing FRP systems to repair and strengthen reinforced concrete (RC) and prestressed concrete (PSC) girders has limitations. Similarly, very few resources address solutions for the debonding problem associated with CFRP laminates or the use of CFRP laminates to repair structural members with pre-existing damage. The included experimental program consists of testing both RC and PSC girders with simulated lateral damage and CFRP repairs. A total of 34 RC beams were statically tested under a 4-point loading until failure and had cross-section dimensions of 5" x 10" (14cm x 25.4cm), were 8' long (2.44m), and were reinforced with either #3 or #4 mild steel rebar. 13 PSC girders having cross-section dimensions representing a half-scaled AASHTO type II shape, were 20' long (6.1m), and were prestressed with five 7/16" (11.1mm) diameter low-lax 7-wire strands. Ten of the PSC girders were statically loaded until failure under a 4-point testing setup, but 3 PSC girders were dynamically tested under fatigue loading using a 3-point arrangement. Different configurations of CFRP laminates, number and spacing of CFRP transverse U-wraps, and amount of longitudinal CFRP layers are studied. The results present the flexural behavior of all specimen including load-deflection characteristics, strain characteristics, and modes of failure. Ultimately, results are used to recommend important considerations, needed criteria, and proper design procedures for a safe and optimized CFRP repair configuration.

CHAPTER 1:
INTRODUCTION

1.0 INTRODUCTION

Uncontrollably, concrete structures all over the world are affected by deterioration or damage. The two primary sources of damage experienced by concrete bridge girders are corrosion and vehicle impacts (Kasan and Harries 2009). Additionally, the combination of the two effects has been demonstrated to be significantly critical (Harries 2009). A nationwide survey shows that on average, in the United States between twenty-five and thirty-five bridges are damaged by colliding overheight vehicles every year, in each state (Fu et al. 2003); most of which are impacted multiple times. For example, in NY State thirty-two bridges have been impacted a total of five-hundred-ninety-five times since the mid 1990's (Agrawal and Chen 2008). The high frequency of these occurrences creates a major concern for transportation departments all over the nation regarding the repair of laterally damaged bridge girders.

Throughout history, a multitude of procedures have been developed to restore any structures seriously affected by such influences. Recently, the use of carbon fiber reinforcing polymers (CFRP) for restoring or enhancing the performance of reinforced concrete (RC) and prestressed concrete (PSC) bridge girders has become more commonly accepted. It has proven to be a more desirable solution providing an inexpensive and rapidly applicable repair method which maintains the original configuration and overhead clearance of the structure (Shin and Lee 2003). However, current repair design

specifications report limitations on accurate debonding predictions and designing various laminate configurations (ACI Committee 440 2008). Similarly, most of the published experimental work that addresses external strengthening of concrete girders with composite materials is focused on specimens without preexisting damage. Little investigation has been conducted on repair of impact damaged girders; which is important due to the high frequency of bridge collisions.

The following research investigates the effectiveness of using non-prestressed CFRP fabric laminates in repairing both RC and PSC girders damaged by lateral impacts that cut through the steel reinforcements and/or prestressing cables; example in Figure 1. Included in the investigation is an evaluation of the proper configuration, size, and spacing of CFRP U-wrappings to mitigate the debonding problem. Other repair application and design considerations such as reinforcement ratio, level of strengthening (number of CFRP soffit layers), development length, and continuity are also addressed in the experimental program and the resulting recommendations are ultimately presented.

Figure 1-1: *Example of overheight impact damage to prestressed concrete bridge girder*

1.1 BACKGROUND

Currently there exists a multitude of options for viable methods to repair structurally deficient reinforced concrete and prestressed concrete bridge components. The use of externally bonded carbon fiber reinforcing polymers (CFRP) to repair bridge girders has proven to have numerous advantages in comparison to traditional methods. CFRP has a high strength to weight ratio, is resistant to chemicals, and the repair methods are usually inexpensively and rapidly applicable in the field with little to no disturbance to traffic; the repairs also maintain the overheight clearance and original configuration of the structure (Shin and Lee, 2003). Yet, in spite of their benefits, the use of externally bonded FRP systems is hampered by the lack of nationally accepted design specifications for their use in the repair and strengthening of concrete bridge elements (NCHRP R-655, 2010).

The current national specifications for designing externally bonded CFRP laminates is the ACI 440.2R-08. This document provides a large array of guidelines for strengthening structural members. However, it does indicate some limitations in its contents and refers to durability and debonding behaviors as “areas that still require research”. It continues to state specifically that “more accurate methods of predicting debonding are still needed” (ACI Committee 440 2008). Similarly, this document also does not provide deflection provisions specific for FRP-strengthened RC beams but instead refers the designer to ACI 318-99 which does not address post yielding deflections for strengthened beams (Charkas et al. 2003).

The ability of bonded CFRP to enhance the capacity of RC or PSC girders is well established with conservative documents such as the ACI 440 reporting enhancement

possibilities up to 160% and multiple independent research papers reporting enhancements up to 200% including Ramana et al. 2001, Grace et al. 1999, and Grace et al. 2003. However, these documents and most others do not address strengthening concrete members with existing damage. In addition, of the papers that do address the repair of damaged members, most are field studies, leaving research conducted in a laboratory setting to describe the overall behavior of impacted girders even more sparse. Furthermore, none of the design references and very few research papers address the effects of intermediate transverse anchoring and the corresponding design considerations. Therefore, with the limitations or lack of research and nationally accepted design specifications it was determined that more investigation was required to develop an efficient CFRP repair design procedure for laterally damaged concrete bridge girders.

1.2 STATEMENT OF HYPOTHESIS

It was believed that by executing an extensive experimental study evaluating the flexural behavior of both reinforced concrete and prestressed concrete beams having simulated lateral damage and various CFRP repairs, the needed design considerations and calculations can be recommended to constitute a safe and efficient repair configuration for concrete girders impacted by overheight vehicles. In particular, through the process of testing, if the effects of intermediate transverse U-wrappings on the strain that is developed in the longitudinal laminates was better understood, unwanted debonding failures could be better predicted and mitigated; resulting in more efficient CFRP repair designs.

1.3 OBJECTIVES

The investigative intent behind the research project is to conduct a cohesive experimental analysis into the feasibility and performance of an innovative repair using CFRP laminates to restore and enhance the flexural capacity of laterally damaged RC and PSC bridge girders. Specific objectives for the research program are to investigate experimentally and analytically the repair performances and their potential debonding, the effectiveness of transverse U-wrappings to mitigate the longitudinal CFRP debonding problem, the optimum configuration of transverse U-wraps, and to develop criteria for the proper number and spacing of transverse U-wrappings for different girder sizes and spans.

The main parameters investigated in the experimental program are:

1. Proper number of longitudinal CFRP laminates (strengthening level)
2. Most efficient spacing of the transverse CFRP U-wrappings.
3. Optimum number of the transverse CFRP U-wrap.

CHAPTER 2:
LITURATURE REVIEW

2.0 LITURATURE REVIEW

The reviewed material covers multiple aspects pertaining to the conducted research presented in this thesis. The referenced documents that follow include national specifications, national experimental research papers, state conducted research investigations, and university conducted research reports.

2.1 BRIDGE IMPACT STUDIES AND ASSESSMENTS

One of the most influential publications investigating damaged PSC bridges was published in 1980 by Shannafelt and Horn. In this report, known as *NCHRP Report 226*, an extensive compilation of statistics provided by cooperating states is presented documenting damaged PSC bridges all over the nation. It is reported that of the 23,344 PSC bridges in those participating states, an average of 201 were damaged each year. Furthermore, it was discovered that 80 percent of the damage to the PSC bridges was due to overheight vehicle collisions. Similarly, more recent studies have been conducted in the same manner to evaluate the frequency of current PSC bridge conditions. In 2003 Fu, Burhouse, and Chang published a study of overheight vehicle collisions reporting that of the 29 state departments participating, 62% considered overheight vehicle collisions a significant problem; including Florida. Additionally, it was stated that on average, between 25 and 35 PSC bridges are damaged each year, in every state. Furthermore, in 2008 Agrawal and Chen reported that, of the bridges that are damaged by overheight

collisions each year many are impacted multiple times. Providing an example in NY State where 32 bridges have been struck a total of 595 times since the mid 1990s.

The resulting statistics from these surveys produced the understanding that there was a need to standardize a method to evaluate damaged PSC bridge members and possible associated repair methods. Shannafelt and Horn followed up their previous investigation with a second publication in 1985 researching the appropriate repairs for different amounts of damage; it is known as *NCHRP Report 280*. This document classified possible damages into three categories.

> Minor Damage: which is defined as; concrete with shallow spalls, nicks and cracks, scraps and some efflorescence, rust or water stains. Damage at this level does not affect a member's capacity. Repairs are for aesthetic or preventative purposes.
>
> Moderate Damage: will include; larger cracks and sufficient spalling or loss of concrete to expose strands. Moderate damage does not affect a member's capacity. Repairs are intended to prevent further deterioration.
>
> Severe Damage: is classified as; any damage requiring structural repairs. Typical damage at this level includes significant cracking and spalling, corrosion and exposed and broken strands.

The repair methods experimentally tested by Shannafelt and Horn investigated external post-tensioning, externally bonded reinforcing bars, mild steel external sleeves, and internal strand splicing. However, in 2009 Kasan published a similar updated study

which sub-divides the "Severe Damage" classification into three different categories and introduces FRP systems as repair methods. The three categories proposed to represent the "Severe Damage" classification are:

> Severe I: the experienced damage requires structural repair that can be affected using a non-prestressed or post-tensioned method. This may be considered as repair to affect the strength (or ultimate) limit state.
>
> Severe II: the experienced damage requires structural repair involving replacement of prestressing force through new prestressing or post-tensioning. This may be considered as a repair to affect the service limit in addition to the ultimate limit state.
>
> Severe III: the experienced damage is too extensive. Repair is not practical and the member or element must be replaced.

The author continues to provide the appropriate or best fitting repair method for a variety of experienced amount of damage; including additional CFRP repair system methods ranging from preformed CFRP strips to non-prestressed CFRP fabrics, near surface mounted (NSM) CFRP, prestressed CFRP, or post-tensioned CFRP. This information is presented and available in Table 1 on the following page.

Table 2-1: Levels of experienced damage and repair methods matrix for pros and cons comparisons (Kasan, 2009)

Damage Assessment Factor	Repair Method								
	Perform CFRP strips	**CFRP fabric**	**NSM CFRP**	**Prestressed CFRP**	**PT CFRP**	**PT Steel**	**Strand Splicing**	**Steel Jacket**	**Replace Girder**
Damage that may be repaired	Severe I	low Severe I	Severe I	Severe II	Severe II	Severe II	low Severe I	Severe II	Severe III
Active or Passive repair	passive	passive	passive	marginally active	active	active	active or passive	active or passive	n/a
Applicable beam shapes	all	all	IB, limited otherwise	all	all	all	IB, limited otherwise	IB	all
Behavior at ultimate load	excellent	excellent	excellent	excellent	excellent	excellent	excellent	uncertain	excellent
Resistance to overload	limited by bond	limited by bond	good	limited by bond	good	excellent	excellent	uncertain	excellent
Fatigue	limited by bond	limited by bond	good	limited by bond	excellent (unbonded)	excellent	poor	uncertain	excellent
Adding strength to non-damaged girders	excellent	good	excellent	excellent	excellent	excellent	n/a	excellent	n/a
Combining splice methods	possible	possible	unlikely	possible	good (unbonded)	good	excellent	excellent	n/a
Number of strands spliced	up to 25%	limited	limited by slot geometry	up to 25%	up to 25%	up to 25%	few strands	up to 25%	unlimited
Preload for repair	no	no	no	no	no	no	possible	possible	n/a
Preload for patch	possible	no	yes	possible	possible	possible	yes	no	n/a
Restore loss of concrete	patch prior to repair	patch prior to repair	patch prior to repair	patch prior to repair	patch prior to repair	patch prior to repair	excellent	patch prior to repair	n/a
Constructability	easy	easy	difficult	difficult	moderate	moderate	difficult	very difficult	difficult
Speed of repair	fast	fast	moderate	moderate	moderate	moderate	fast	slow	very slow
Environmental impact of repair	VOC's from adhesive	VOC's from adhesive	adhesive VOC's & dust	VOC's from adhesive	minimal	minimal	minimal	welding	erection issues
Durability	environmental protection	environmental protection	excellent	environmental protection	environmental protection	corrosion protection	excellent	corrosion protection	excellent
Cost	low	low	moderate	moderate	moderate	low	very low	moderate	high
Aesthetics	excellent	excellent	excellent	excellent	fair	fair	excellent	excellent	excellent

2.2 DESIGN CRITERIA AND EXISTING CODES

Since the emergence of CFRP usage as a structural repair or enhancement, efforts have been made to standardize both the predicted behaviors and needed design calculations for implementation. The ACI440.2R-08 addresses the design criteria and calculations for designing externally bonded CFRP systems to repair both RC and PSC bridge girders. However, the ACI document indicates some limitations in its contents and refers to durability and debonding behaviors as "areas that still require research". It continues to state specifically that "more accurate methods of predicting debonding are still needed". Furthermore, this document also does not provide deflection provisions specific for FRP-strengthened beams but instead refers the designer to ACI 318-99 which does not address post yielding deflections for strengthened beams (Charkas et al. 2003). Similarly, the AASHTO and AASHTO LRFD provisions (which provide specifications for structural design parameters including design loading criteria, impact factors, and reduction factors) do not contain appropriate values or calculations for concrete members strengthened with CFRP laminates.

Some of the aforementioned limitations have been previously addressed by other researchers. El-Tawil and Okeil developed a fiber section model that accounts for inelastic material behavior, composite action between deck and girder, CFRP bonding properties, and various parameters involved with the construction sequence. Using this model to conduct thousands of Monte Carlo simulations the pair ultimately proposes an equation for the flexural strength reduction factor for PSC girders strengthened with CFRP in their 2010 publication. Likewise, Charkas, Rasheed, and Melhem present a rigorous procedure for accurately calculating the deflections of RC beams strengthened

with FRP systems. Their method of calculation is based on a moment curvature relationship which is idealized to be trilinear addressing precracking, post-cracking, and post-yielding stages. Lastly, a 2008 publication by Rosenboom and Rizkalla investigates the common debonding problem associated with bonded CFRP laminates. This document identifies and discusses the most common premature debonding concern, referred to as intermediate crack (IC) debonding. This is where the crack propagations through the interface of the bond are initiating at the toes of intermediate flexural cracks. Through experimental testing and analysis they first provide evidence that the current calculation modes do not correlate. Then, ultimately a discussion is provided regarding a more accurate proposed model for IC debonding predictions.

2.3 MATERIAL PROPERTIES AND BENEFITS

Since the emergence of interest in using FRP products to restore/retrofit structural components a great deal of research has been done to evaluate benefits of both the material and the cost of implementation. The resulting consensus from the industry is that FRP products and the applications in which they are implemented are much more desirable methods for repairing or restoring degradated structural components. In agreement with many other documents, Shin and Lee use a good description in their 2003 publication stating that, with CFRP's high strength to weight ratio, it's resistance to chemicals, and it's ease of application, inexpensive and rapid restorations can be implemented in the field with little to no disturbance to traffic flow while maintaining the structure's original configuration and overheight clearance. Similar praises of the material's effectiveness after application have also been documented; R. Alrousan reports

that the use of CFRP composites used to rehabilitate structural components can greatly reduce maintenance requirements, increase life safety, and increase the service life of the overall structure. Likewise, as Meisam Gorji points out in his 2009 publication, the properties and behaviors of CFRP materials are so effective for repairing structures it has been intensely used by aerospace agencies on extraterrestrial structures.

In addition to benefits of the material properties, it is also commonly reported that the cost benefits are much desired also. Though it should be known that CFRP materials do carry a hefty price tag, application/labor costs are so greatly reduced that it becomes effective. In 1999, Grace et al. makes a comparison and concludes that in combination with the savings in the repair cost and the elimination of future maintenance cost FRP applications are economically competitive with their steel counterparts.

However, the intent of the included research is specifically geared towards non-prestressed fabric CFRP repair applications; whereas the previous statements above are directed towards the benefits of FRP applications in general. Kasan and Harries addressed these aspects in their 2009 document by concluding that even though it has been demonstrated that prestressed and post-tensioned CFRP repairs utilize the carbon fiber material more efficiently, the difficulties and cost of implementation are more significant than the cost of extra CFRP material needed for non-prestressed applications.

2.4 FLEXURAL REPAIR DESIGNS AND CONSIDERATIONS

Initiating a discussion concerning the design considerations for implementing an efficient structural repair using non-prestressed fabric CFRP laminates it seems logical to start with the considerations addressed by the current American standards for the design

of externally bonded FRP systems. This reference is the ACI 440.2R-08 already previously mentioned; and appropriately, one of the first considerations it addresses is the scope and limitations of implementing various FRP repair systems. Each FRP repair system, whether it is prestressed FRP, post-tensioned FRP, non-prestressed FRP, or near surface mounted FRP bars, has its own abilities and limitations. This is why the ACI document first advises the execution of a detailed and thorough condition assessment of the existing structure which is to receive the repair or retrofit. The primary information that should be established during the assessment includes the existing load-carrying capacity of the structure, any structural deficiencies and their causes should be identified, and the condition of the concrete substrate should be determined. The document continues further and elaborates, recommending that a multitude of items be determined. These items include, the existing dimensions of the structural members; the location, size, and causes of cracks and spalls; the location and extent of any corrosion of reinforcing steel; the presence of any active corrosion; the quality and location of existing reinforcing steel; the in-place compressive strength of the concrete; and the soundness of the concrete, particularly the concrete cover in all areas where the FRP system is going to be bonded to the concrete.

The second major consideration raised by the ACI document is the strengthening limitations that should be followed to prevent sudden failure of the repaired member in case the FRP system is damaged. The philosophy of the guidelines used to specify these strengthening limitations is that a loss of the FRP system should not cause member failure under a sustained service load. These imposed limitations are specific to each repair project and should consider aspects such as the calculated load limitations, the

rational load paths, effects of the temperature and environment on the FRP system, and any effects of reinforcing steel corrosion on the repair. The document further discusses the importance of these considerations and limitations as they relate to fire codes because FRP materials are known to degradate under high temperatures. The degradation of the material is to the point that, in the instance of fire the FRP system is usually assumed to be completely lost.

Other design aspects mentioned in the document that should be considered relate to the installation of the FRP system. The first aspect related to installation addressed is substrate repair and surface preparation. Where, in the case of bonded fabric CFRP, it recommends that all problems associated with the substrate should be repaired; including both corrosion-related deterioration in the substrate and crack control/crack injection. Similarly, in the case of bond-critical applications such as CFRP fabrics, a number recommendations are made related to surface preparation that facilitate a strong bond between the FRP material and the concrete surface. The recommendations related to the surface preparation include, but are not limited to: rounding off any sharp outside corners of the member; cleaning the surface so it is free of any dust, dirt, oils, or anything else that could interfere with the bond of the FRP system; filling in any variations that could cause voids between the two materials, such as extrusions or bug holes, with an approved putty material; and lastly, the repaired surface should be roughly grinded or sanded to help insure an adequate bond. The design aspects related to the installation that address the FRP material itself include considerations such as the alignment of the FRP materials, lap splices used when multiple layers are applied to a member, and temporary protection needed during the curing process of the resins used to bond FRP materials to concrete.

Lastly, the quantified design considerations for flexural strengthening calculations are detailed in chapter ten of the ACI document. This chapter first gives a reasonable range of increases in flexural strength from 10 to 160% which was adopted from other supporting documents. It continues to describe verbally and mathematically the required aspects of its recommended strength design approach. The aforementioned aspects include the nominal strength considerations as they would pertain to each failure mode, the assumptions used when designing repairs for either reinforced concrete or prestressed concrete members, shear strength requirements, existing substrate strains, strain and stress levels that are developed in the FRP reinforcements, strength reduction factors that could be applicable, serviceability design requirements, creep-rupture and fatigue stress limits, stresses developed in steel reinforcements under service loads, and the ultimate strength of the designed repair section. To summarize, the document provides guidance on proper detailing and installation of FRP systems to strengthen and repair structural members to prevent any undesirable failure modes. Though the ACI document includes a vast number of design considerations and calculations the limitations which it contains, previously described in section 2.2, and considerations not mentioned in the document have been researched by several independent entities.

Most all are in general agreement with the ACI, documenting the ability of CFRP to increase the capacity of a bridge girder by gaining maximum enhancements around 200% as reported in Ramana et al. 2001, Grace et al. 1999, and Grace et al. 2003. Similarly, the ACI 440.2R-08 concludes that debonding behaviors will require more research, and many investigative efforts resulted in the same conclusion; *Di Ludovico et al. 2005, Green et al. 2004*, and *Klaiber et al. 1999* all report issues with premature

debonding failures due to either inadequate transverse CFRP anchors or development lengths. Though several papers report debonding issues, a number of conducted researchers have demonstrated successful cases of repairing damaged bridge girders. As a result the general conclusions accepted to constitute a satisfactory are summarized well in a 1999 publication by Grace et al. which states that by providing both horizontal and vertical FRP laminates coupled with the proper epoxy can decrease the deflection and possibly double the ultimate carrying capacity of a repaired girder. They continue to state that the vertical layers are used to prevent rupture or early debonding failures in the flexural horizontal laminates.

Then, in more recent publications by Rosenboom et al. the design issues concerning the presents of lateral damage which cut through prestressing reinforcements on one side of the girder is addressed. In their 2010 publication they present a study of five laterally damaged full-scale AASHTO type II girders repaired with CFRP tested under both static and fatigue loading. Concluding the research it was determined that PSC girders having a significant loss of concrete cross-section and up to 18.8 percent loss of prestressing can be repaired using CFRP laminates to restore the original capacity of the member. It continues to suggest that detailing of the CFRP repair configuration should be carefully considered to restrain the opening of cracks in the damaged region and to prevent debonding; which in their research included a longitudinal laminate on the side of the bottom flange of the girders. Other conclusions provided information into fatigue and shear behavior, claiming that AASHTO girders repaired with CFRP can withstand over 2 million cycles of fatigue loading with very little degradation and the ACI 440 document provides accurate predictions to the shear behavior of the section.

As for the implications that the established shear design aspects are already very accurate for designing CFRP laminate repairs, this has been proven and documented in several studies and therefore will not be addressed in the following conducted research. However, the same does not apply for the fatigue implications raised in the publication by Rosenboom et al.

In a previous study by Rosenboom and Rizkalla they state that "The effect of the CFRP strengthening on the induced fatigue stress ratio in the prestressing strands during service loading conditions is not well defined." (Rosenboom & Rizkalla, 2006) Yet, in a 2001 publication by El-Tawil et al. it was concluded that fatigue cycle loading leads to a redistribution of stresses similar to that obtained under static creep. They specify that the stresses in the steel can display an increase in stress of approximately five percent due to fatigue cycling. They follow up by recommending a limitation that the service steel stresses should not exceed eighty-five percent of the yield strength to account for the increase in stress displayed, shrinkage, creep under dead loads, and any variability in the reinforcing steel strength. Though there exists some conflicts between some previous researches there seems to be a general agreement that CFRP repairs can sustain increased load levels under fatigue cycling.

CHAPTER 3:
EXPERIMENTAL STUDY

3.0 EXPERIMENTAL STUDY

The experimental study included the static flexural testing of 34 reinforced concrete (RC) beams, static flexural testing of 10 PSC girders, and dynamic fatigue testing of 3 prestressed concrete (PSC) girders. The static loading was applied using a 4-point loading arrangement, whereas the dynamic testing was conducted with a 3-point arrangement. As for the test specimen, other than the control samples, simulated lateral damage was imposed and various CFRP repair configurations were applied to all beams. Multiple load measurements, deflection measurements, and strain measurements were recorded at various locations during testing. Similarly, modes of failure and observed behaviors were also documented during loading.

3.1 Reinforcing Materials

The CFRP product decided upon for the research was the Fyfe-Tyfo® SCH-41, a uni-directional carbon fiber fabric. It was used in conjunction with the Tyfo® S Saturant, an epoxy designed by the manufacturer specifically for the CFRP product. This product was selected based local availability and the properties and outcomes reported in previous research; a picture of the material is presented in Figure 3-1 and all design values for the reinforcement properties are listed in Tables 3-1 and 3-2.

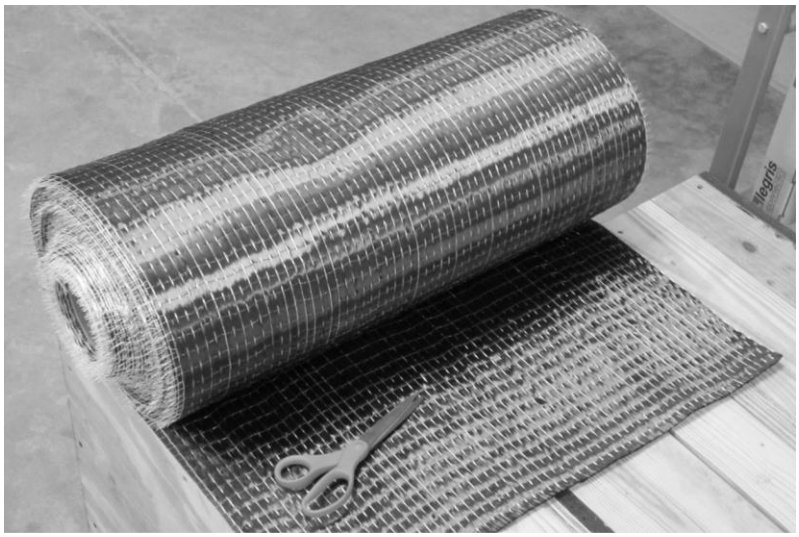

Figure 3-1: Picture of Carbon Fiber Fabric Material Used on Test Specimen

Table 3-1: Carbon Fiber Laminate Design Properties

FYFE-Tyfo SCH-41 Composite CFRP using Tyfo S Epoxy						
CFRP Material Properties	Tensile Strength	Tensile Modulus	Ultimate Elongation	Density	Weight per Sq yd.	Nominal Thickness
Typical Dry Fiber	550,000 psi 3.79 GPa	33.4 x 10^6 psi 230 Gpa	1.70%	0.063 lbs/in^3 1.74 g/cm^3	19oz. 644 g/m^2	N/A
*Composite Gross Laminate	121,000 psi 834 MPa	11.9 x 106 psi 82 GPa	0.85%	N/A	N/A	0.04 in 1.0 mm
*Gross laminate design properties based on ACI 440 suggested guidelines will vary slightly						

Table 3-2: Mild Steel Design Properties

Steel Reinforcement Material Properties							
Bar Number	Dia.	Bar Area	grade	Youngs Modulus	Weight	Yeild Strength	Ultimate Strength
steel wire cage	0.072 in 1.83 mm	0.004 in^2 2.63 mm^2	60	29x10^6 psi	0.014 lbs/ft	60,000 psi 345 N/mm^2	90,000 psi 621 N/mm^2
#3 bars	0.375 in 9.53 mm	0.11 in^2 71.3 mm^2	60	29x10^6 psi	0.376 lbs/ft	60,000 psi 345 N/mm^2	90,000 psi 621 N/mm^2
#4 bars	0.5 in 12.7 mm	0.2 in^2 126.7 mm^2	60	29x10^6 psi	0.683 lbs/ft	60,000 psi 345 N/mm^2	90,000 psi 621 N/mm^2

3.2 TEST SPECIMENS

3.2.1 Reinforced Concrete Beams

Two sets of RC specimens were designed; both were 8.0ft (2.44m) long with cross-section dimension of 5.5in by 10.0in (14cm by 25.4cm). A grade 60 steel wire mesh having verticals of 0.072in (1.83mm) diameter spaced every 4 inches (10.2cm) was provided in both sets as shear reinforcements. The first set "TB" contained three #4 mild steel rebar (grade 60) evenly spaced with a bottom cover of 1.5in (3.8cm) and the second set "JB" contained three #3 (grade 60) mild steel rebar evenly spaced with the same cover. Figure 3-2, presents a sketch of the designed cross-sections.

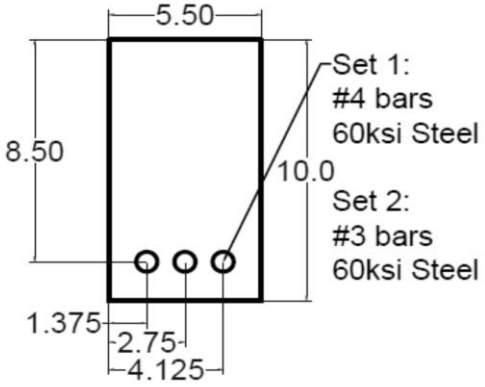

Figure 3-2: Cross-section Dimensions (inches) of RC Test Sample

The imposed simulated damage was implemented by cutting and bending one of the reinforcing rebar at mid-span prior to casting. Then, by casting the concrete around the damaged reinforcement, the condition of the beams represented a scenario of a member that has undergone lateral damage and received a perfect concrete repair. Figure 3-3 shows examples of the RC beam forms and the cut and bent rebar.

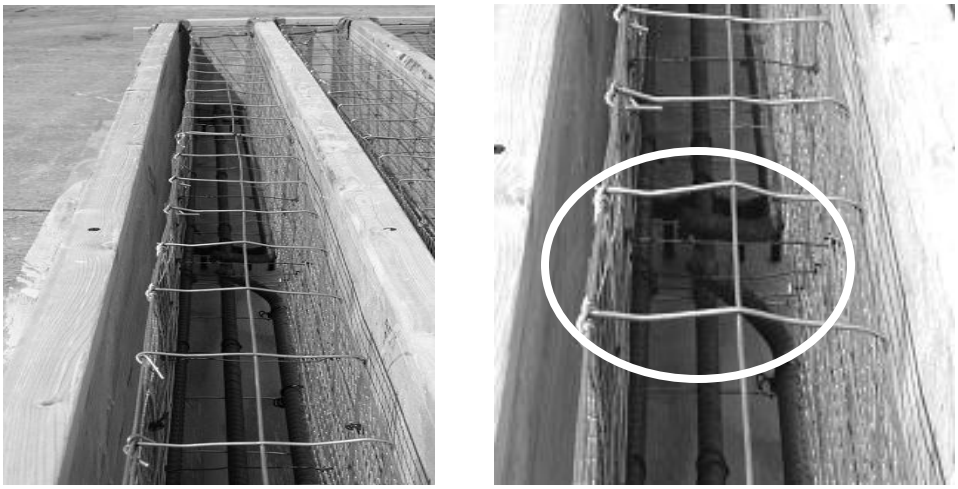

Figure 3-3: (left) Wood forms and reinforcements; (right) Simulated damage

The designed concrete strength for both RC sets was 5,500psi (37.9MPa). Yet, on the day of the pours, multiple 3in x 6in (76.2mm x 152.4mm) compression cylinders were cast in addition to the RC beams and the actual average concrete compressive strengths for each set was evaluated by breaking the cylinders on the day of the beam testing. The first set "TB" had an average compressive strength value of 6,943psi (47.87MPa) and the second set "JB" had an average value of 7,834psi (54.01MPa).

3.2.2 PSC Girders

The PSC girders tested were 20ft (6.1m) long and had cross-sectional dimensions representing a half-scale model of an AASHTO type II girder. An additional decking 4in (10.16cm) thick was also cast on top of the girders to simulate a bridge deck composite with the PSC girder. The concrete used for manufacturing the girders ended up having a compressive strength of approx. 10,000 psi (68.9 MPa) on the days of testing, though it was specified to be designed at 6,500 psi (44.82 MPa). A total of five low-relaxation grade 270 seven-wire prestressing strands were used to reinforce each girder. In addition, three 60ksi (413.7MPa) non-prestressed rebar were provided

in the girder flanges and two rebar in the deck topping. Half of the steel stirrups, provided for shear, extended vertically from the girder to the decking while the other half remained entirely in the girder. They were spaced every six inches alternating between the two height sizes, providing nearly the maximum amount of shear reinforcement for the cross-section. The girders were designed to be heavily reinforced in shear in order to avoid any premature failures which could jeopardize the test results and the investigations into the debonding issues. Figure 3-4 presents a diagram of the cross-section and the reinforcements.

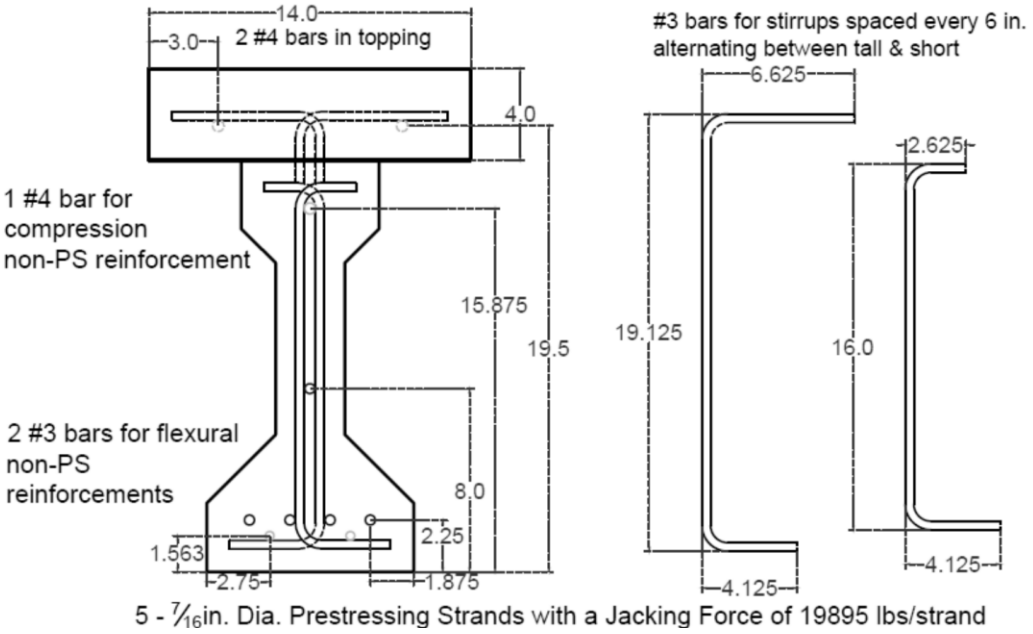

Figure 3-4: Half-scaled AASHTO type II cross-section and reinforcements

The lateral damage simulation was achieved by saw cutting through the concrete at the bottom flange of each girder and slicing through one of the prestressing strands. A schematic of this procedure and a picture of the resulting cut are shown in Figure 3-5. To repair the cut, the opening left from the saw was first roughened up using chisel tools to help improve the bonding area. The surface of the concrete exposed by the

cut was then thoroughly cleaned with a water jet and pressurized air. The cleaned opening was filled with a high strength cementitous repair mortar and a high pressure epoxy injection procedure was performed after the mortar set (Figure3-6). The procedure resulted in a near perfect repaired cross-section, as seen in Figure 3-7.

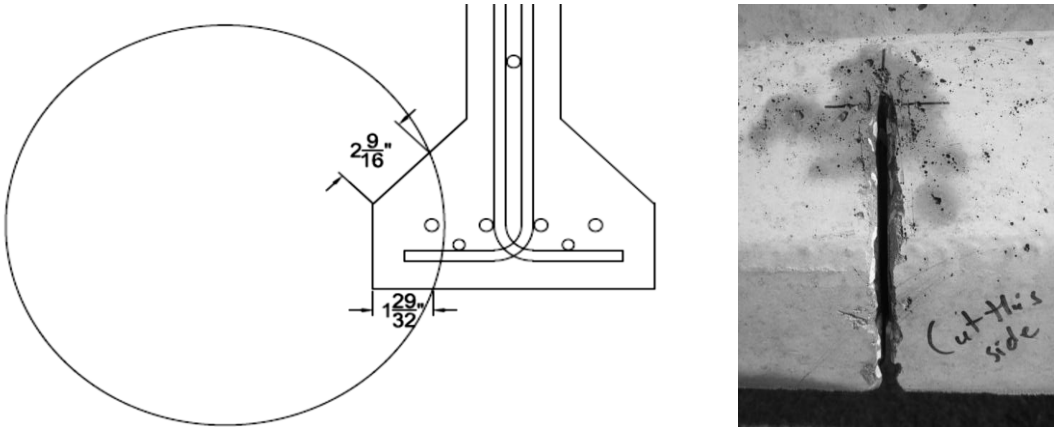

Figure 3-5: (left) Diagram of saw cutting used to simulate damage in the girders; (right) Photo showing resulting cut in actual girder sample

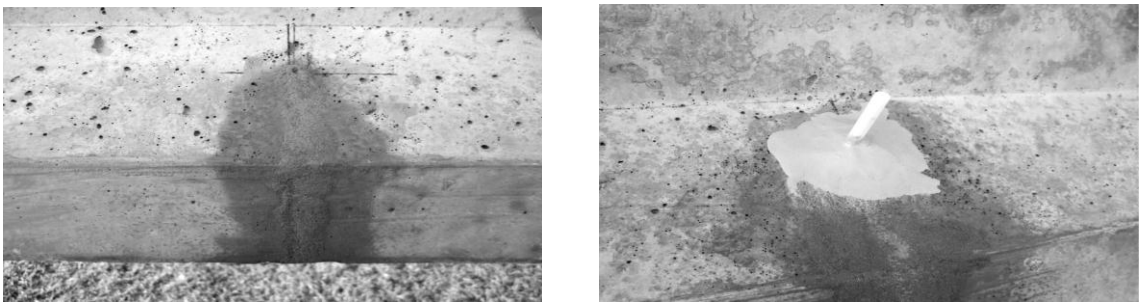

Figure 3-6: (left) Saw cut filled with repair mortar; (right) Injection port for epoxy injection

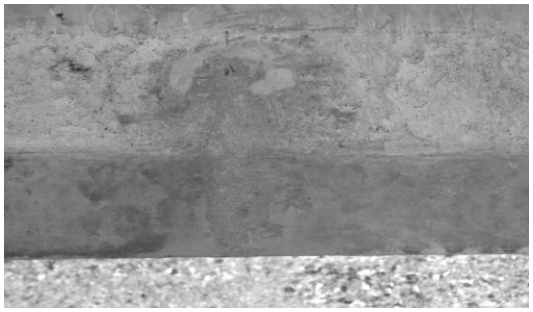

Figure 3-7: Finished repaired section

3.3 CFRP REPAIR CONFIGURATIONS

All major repair design considerations for the CFRP were decided upon based on the methodology described in the ACI440.2R-08 which utilizes conventional Whitney stress block factors. Similarly, all repairs were applied using the wet layup method which is discussed with detail in section "3.4 CFRP Repair Application Process". This procedure was preferred, as it is most commonly used for its low cost and high structural effectiveness (Rosenboom et al. 2007).

3.3.1 RC Beams

The first set "TB", containing fifteen beams, was cast at the FDOT lab facilities in Tallahassee, Florida. This set of beams contained the #4 steel rebar for flexural reinforcements. The control beams without a cut rebar had a reinforcement ratio (ρ) of 0.0128 and the damaged beams, with a cut rebar, had a reinforcement ratio of 0.0085**.** Each beam in this set receiving CFRP was repaired with one longitudinal layer of 4in (10.2cm) wide, 0.04in (1.0mm) thick CFRP laminate bonded to the beam soffit. The U-wrappings applied for the repairs were 4.75in (12.1cm) wide and (0.04 in 1.0mm) thick and they extended to the top fiber of the beams. The spacing distances were also set at a standard of 4.75in (12.1cm) or multiples thereof. Figure 3-8 presents a picture of a set of finished specimens and the various configurations tested for the first set are shown in Figure 3-9.

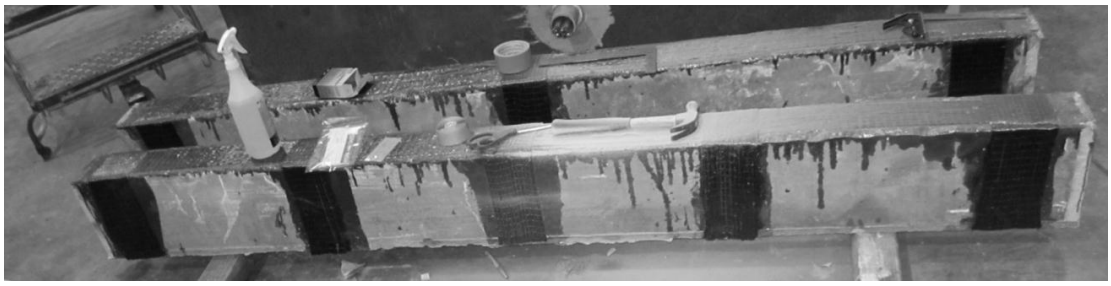

Figure 3-8: Sample of Repaired Reinforced Concrete Test Beams

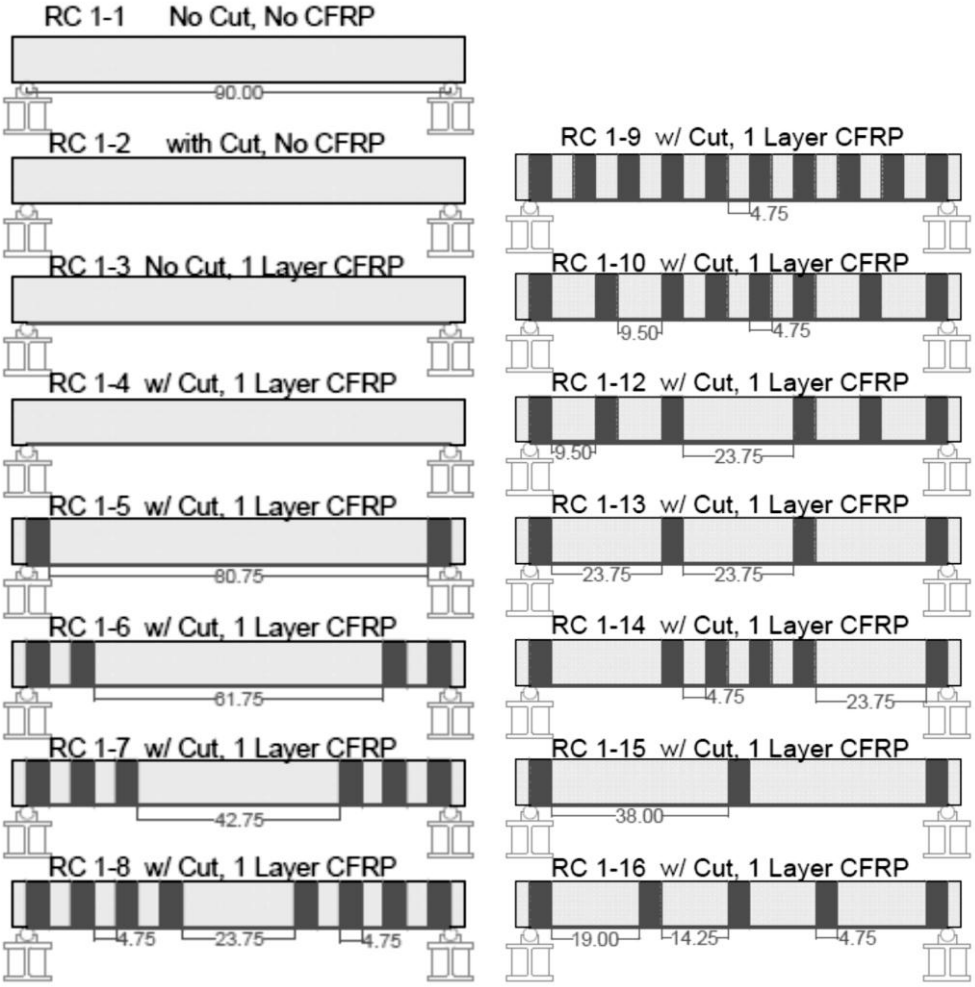

Figure 3-9: First Set ("TB" set) of 15 RC Beams, CFRP Configuration Layouts

The second set "JB" consisting of 19 RC beams was cast at the UNF lab in Jacksonville, Florida. This set contained the #3 rebar for flexural reinforcements and two layers of the 4in (10.2cm) wide CFRP laminates were applied to the soffits. For

this set, the undamaged control beam had a reinforcement ratio (ρ) of 0.0071 and reduced reinforcement ratio (ρ) of 0.0047 for the damaged beams**.** CFRP U-wrap sizes and spacing used was identical to that of the first set. Figure 3-10 shows the configuration layouts for the second set.

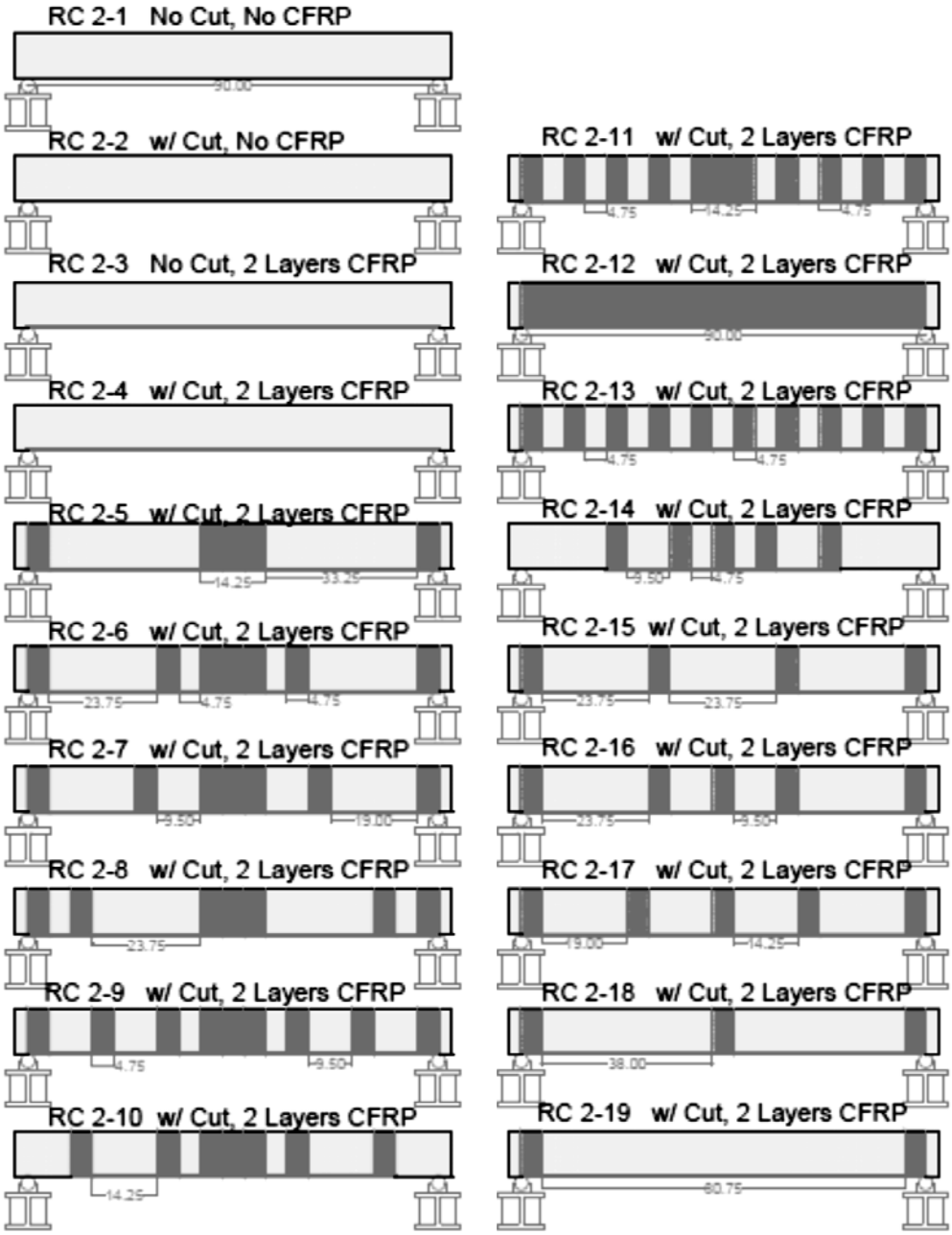

Figure 3-10: Second Set ("JB" set) of 15 Beams, CFRP Configuration Layouts

3.3.2 Statically Tested PSC Girders

Multiple CFRP configurations and strengthening levels were used to repair the ten PSC girders. The longitudinal strips were all eight inches wide and started at seventeen feet long, reducing six inches per each additional layer applied to each beam. The transverse U-wrappings were twelve inches wide and extended to the top of the web of the each girder. Figures 3-11 & 3-12 show the CFRP configurations for the half-scaled AASHTO type II girders statically tested.

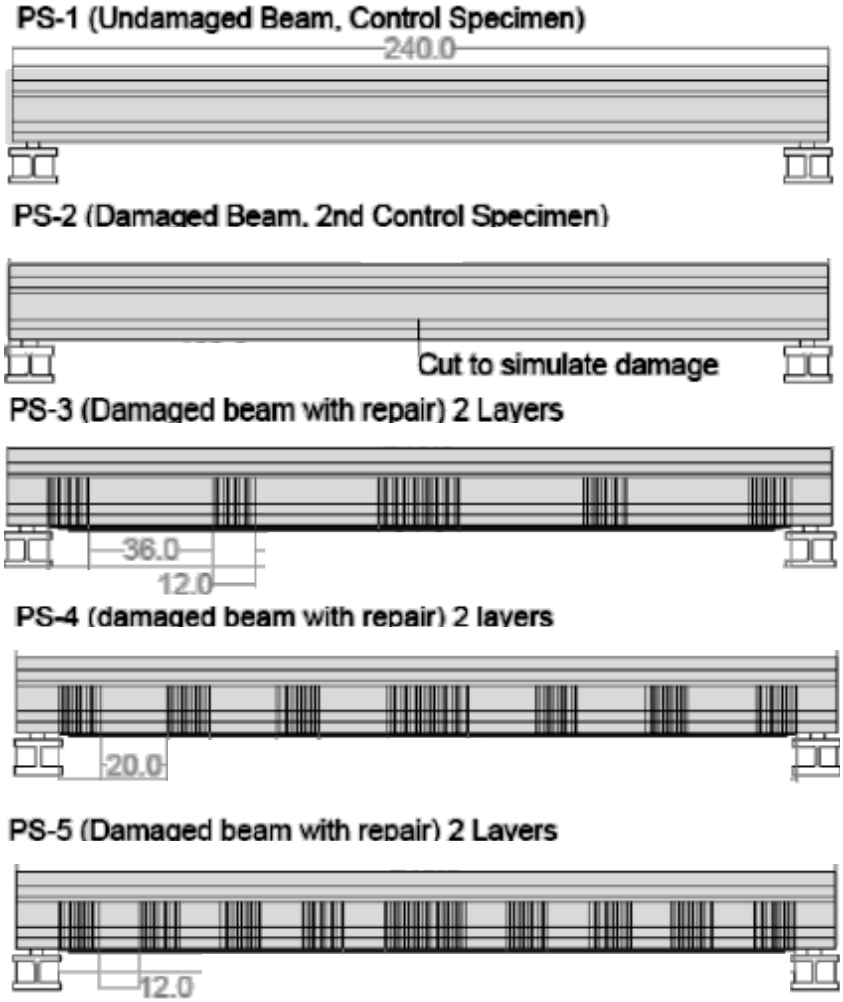

Figure 3-11: First 5 PSC Girders, CFRP Configuration Layouts

In Figure 3-11, the first girder (PS-1) is a control girder that represents an undamaged and unrepaired specimen. Similarly, the second girder (PS-2) is a damaged specimen which has received no CFRP repair (only concrete repair) representing the lower bound of the tested samples. The remaining girders had both simulated impact damage imposed on them and 2 layers of CFRP at various spacing to constitute the repair. The spacing between U-wrappings was set at a distance of twelve inches, twenty inches, or thirty-six inches.

Similarly, Figure 3-12 displays the CFRP configurations for the remaining girders tested. The first three girders presented (PS-6 through PS-8) are damaged and repaired with 3 layers of CFRP at the girder soffit and U-wrappings at the same spacings of twelve inches, twenty inches, or thirty-six inches. The final two beams (PS-9 & PS-10) are fully wrapped girders, having U-wrappings cover the entire beam, using 2 layers of CFRP for both the longitudinal and U-wrapping laminates. However, the U-wrappings applied to PS-10 were overlapped by approximately an inch, whereas those applied to PS-9 were not. This was intended to investigate a simple question of needed continuity in the direction opposite to the direction which the fibers run.

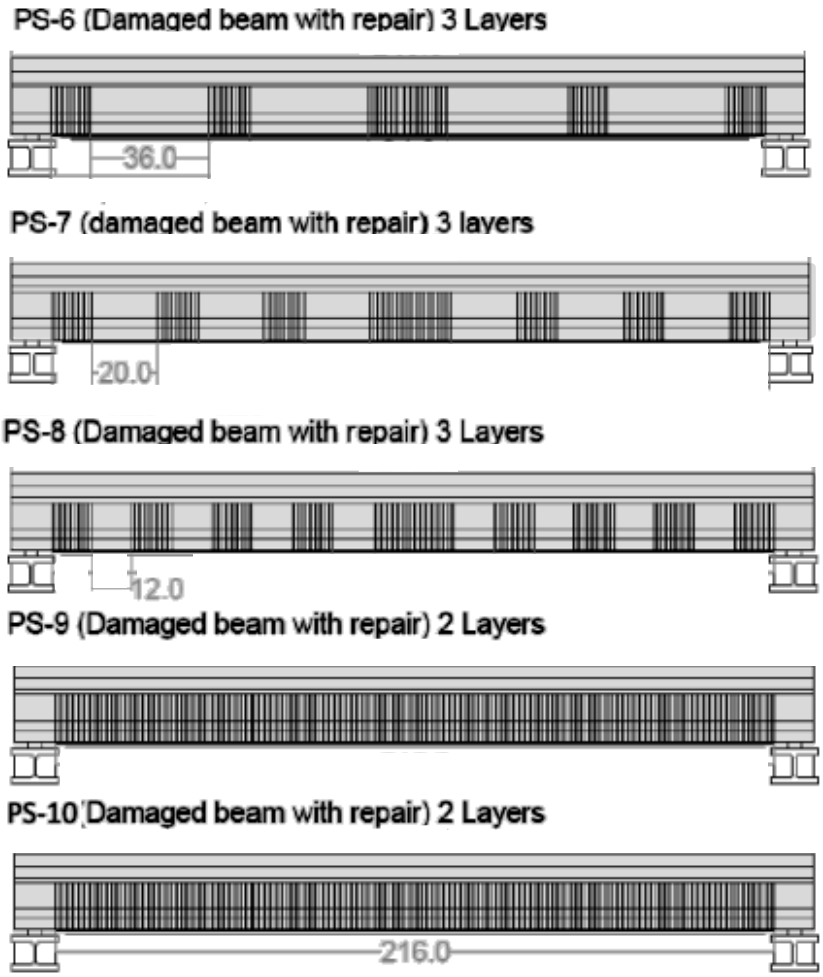

Figure 3-12: Second Set of 15 Beams, CFRP Configuration Layouts

3.3.3 Dynamically Tested PSC Girders

Each of the three girders tested under fatigue loading was designed with a different CFRP configuration. However, in each, all the longitudinal strips were eight inches wide and started at seventeen feet long, reducing six inches per each additional layer applied to each beam. The transverse U-wrappings were twelve inches wide and extended to the top of the web of the each girder. Figure 3-13 shows the CFRP configurations for the half-scaled AASHTO type II girders dynamically tested.

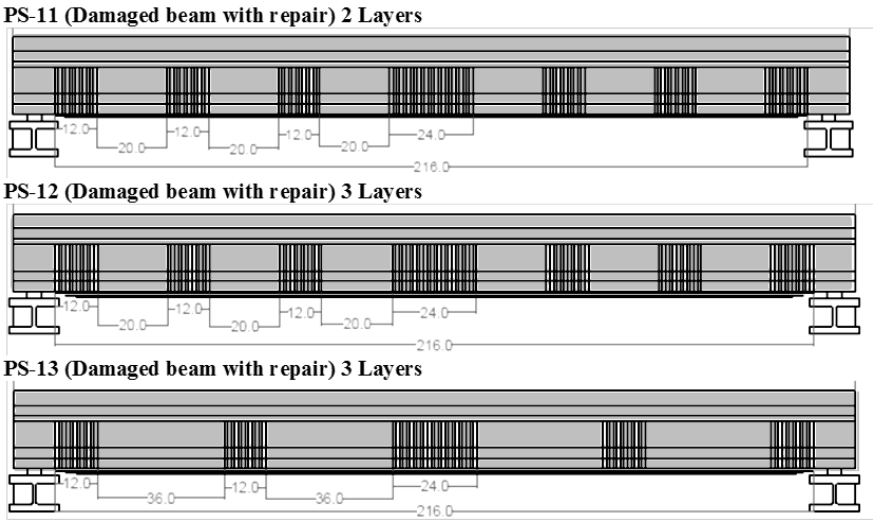

Figure 3-13: CFRP Configurations for Dynamically Tested PSC Girders

Both PS-11 and PS-12 had 20in spacings between transverse U-wrappings; however, PS-12 had three longitudinal layers of CFRP whereas PS-11 only had two. Unlike either, PS-13 had 36in spacings between transverse U-wraps but it did utilize three longitudinal CFRP layers like PS-12.

3.4 CFRP REPAIR APPLICATION PROCEDURES

3.4.1 RC Beams

For both sets of the reinforced concrete specimens, students from the University of North Florida performed the installation procedure in which a simplified wet lay-up procedure was implemented. The beams were first positioned upside-down, fully supported, and then the surfaces were roughened and cleaned. When applying the CFRP repair, first a priming layer of the Tyfo® S epoxy was rolled onto the tension face of the girder where the longitudinal CFRP laminate would be applied. One layer of pre-cut fabric saturated in the same epoxy was then placed on the tension face of the girder and rolled out to remove any air bubbles. A second layer of the epoxy was

then added over top of the applied fabric. If a second longitudinal CFRP layer was required it was added in the same fashion. Similar to the longitudinal procedure, before applying the saturated U-wrappings the concrete surface was first rolled with the epoxy. The U-wrappings were then applied in the same manner as the longitudinal laminates.

3.4.2 PSC Girders

For the prestressed concrete girders, employees of Fibrwrap® performed the installation procedure for the ten statically tested samples in which a traditional wet lay-up procedure was implemented. Their crew first took grinders to the entire surface below the top flange of the girders. Next pressurized air was used to blow the concrete dust from the surfaces and a pressure washer was used to clean the girders. After drying in the sun, pressurized air was blown over the girders again and they began to mix the epoxy. Each portion of the epoxy was split and half was mixed with a substantial amount of Cab-o-Sil® fumed silica in order to gain a more desirable consistency. Figure 3-14 shows the silica product and the resulting thickened epoxy.

Figure 3-14: (left) Fumed Silica used to Thicken Epoxy; **(right)** Thickened Epoxy

Using the original thinner Tyfo® S epoxy a layer was rolled onto the concrete surface of the girders where the CFRP laminates would be applied. A thin layer of the thickened epoxy, containing the fumed silica, was then applied to the tension side of the girders and the first pre-cut longitudinal laminate, saturated in un-thickened epoxy, was attached. Trowels and paint rollers were used to remove any air voids once the first layer was adhered. Next, a second layer of the thickened epoxy was applied on top of the first laminate layer. At this point any required subsequent longitudinal layers were applied in the same manner. This procedure was identically followed for each layer of transverse U-wrapping applied with one added important process. To attach the transverse laminates all bonding procedures were performed on one side first while the remaining fabric hung towards the ground. Then with one side secure, the laminates were pulled tightly to ensure effectiveness as they wrapped around the cross-section. Figure 3-15 provides a moment of the process.

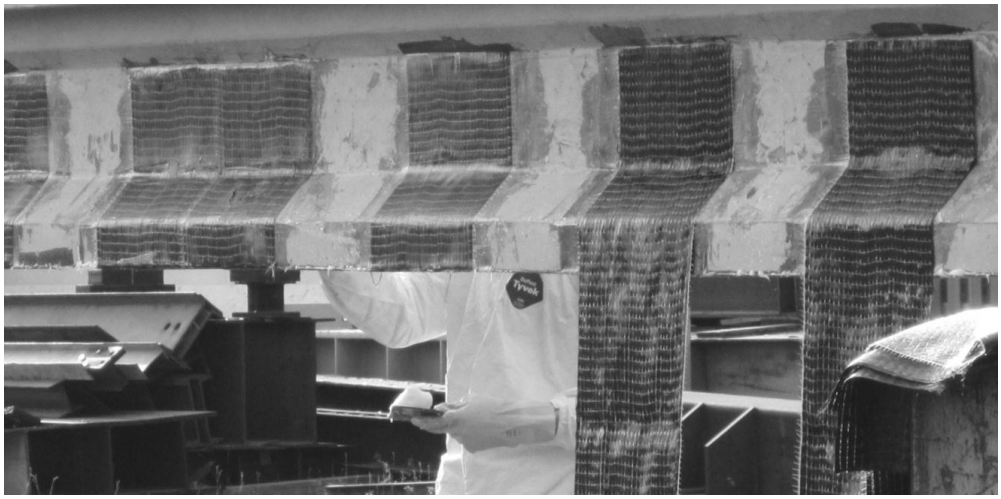

Figure 3-15: Transverse CFRP U-wrappings being applied by FIBRWRAP

Lastly, a final layer of the silica fume thickened epoxy was spread over all CFRP laminates and the outlining concrete surface. In the case of the PSC girders, some

small air voids were found beneath the CFRP laminates after curing and were injected with a similar structural repair epoxy.

3.5 TEST SETUP AND INSTRUMENTATION

All beams reported in this research have been tested at the Florida Department of Transportation (FDOT) structural research center in Tallahassee, Florida under the supervision of state employed engineers and technicians.

3.5.1 RC Beams

The RC beams were tested under a four point loading setup using a 100kip (445kN) load actuator mounted on a steel frame. The 8ft (2.44m) long RC beams spanned 7.5ft (2.29m) between the centerlines of the bearing surfaces and rested on stationary steel cylindrical supports. The four point loading was applied by using a steel spreader I-beam resting on a set of bearing pads with a center to center distance of 20 inches straddling the center line of the beam. In turn, applying half the load at a distance of 10in (25.4cm) off center on each side. Aside from the specimens, the supports, and the loading apparatus, measurement devices were also instrumented for every test and the specifications are included with the test setups.

The beams were instrumented with two laser deflection gages, four linear variable differential transformer (LVDT) deflection gages, and between 4 to 7 strain gages (30 mm long- 120 ohm). The two laser deflection gages were positioned at the center of the beams' span both above and below each beam. Two of the LVDTs were placed on the beams' top surface above the supports and the remaining two LVDTs were placed

on the beams' top surface at quarter points of the beams' span. Figure 3-16 displays a picture of the testing setup for the RC beams.

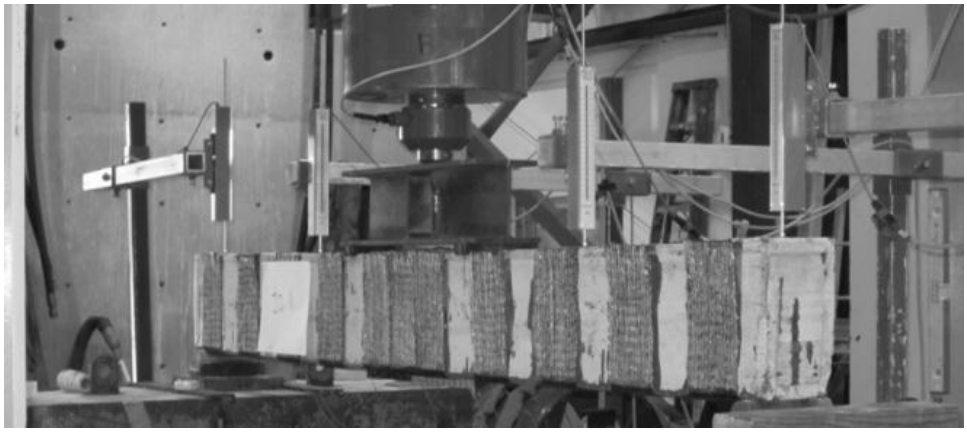

Figure 3-16: Example of Testing Setup for RC beams

Four strain gages were placed along the height of the beam cross-section at mid-span. One strain gage was placed on the very top fiber of the beam, one on the very bottom, the third at the steel level, and the remaining is located halfway between the depth of the steel and the top fiber. The remaining strain gages were distributed along the flexural CFRP laminate on the tension side of the beam. These gages had varying location placements depending on the configuration of the transverse U-wrapping anchors. A schematic of the test setup and layout of the measuring devices is depicted in Figure 3-17.

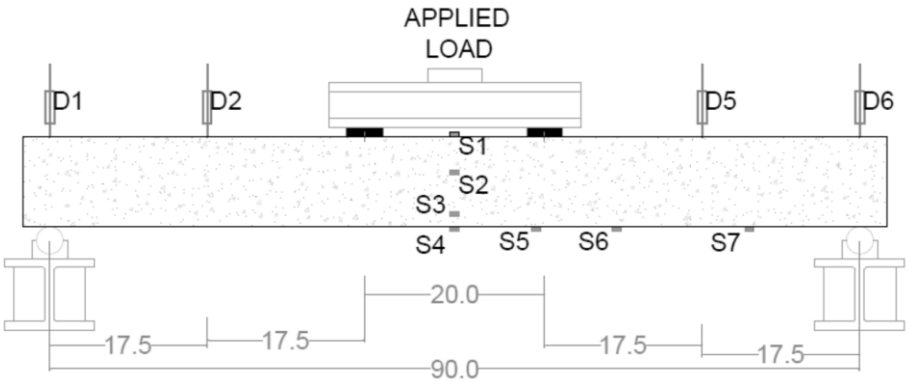

Figure 3-17: RC Samples, Testing Setup Schematic

3.5.2 PSC Girders Statically Loaded

The statically loaded girders were tested under a four point loading arrangement using an 800 kip load actuator at the FDOT structures research lab. The 20-ft long PSC girders spanned nineteen feet between the centerlines of the bearing pads which rested on stationary supports. The girder loading was applied using a steel spreader beam resting on another set of two pads with a center to center distance of fifty inches. Along with the structural arrangement, measurements were recorded through the set-up of many gage devices. Other than load measurements recorded by the actuator, the girders were also instrumented with six LVDT (linear variable differential transformer) deflection gages and up to twelve strain gages (30 mm long-120 ohm). Two LVDT deflection gages were positioned at center span on each side of the girder, two LVDTs were placed at girder top surface above the support areas, and the remaining two LVDTs were placed at quarter points of the girder span. On each girder, four of the strain gages were placed along the height of the cross-section at mid-span and the remaining strain gages were distributed along the flexural tension side at various locations depending on the CFRP configuration. The general placements of all measurement devices mentioned are also shown in Figure 3-18 and a photo of PCS 5 set up for testing is given in Figure 3-19.

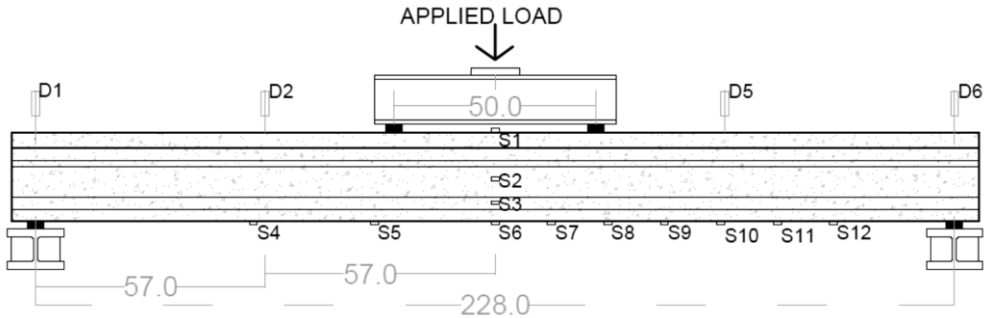

Figure 3-18. Testing Setup Schematic for Statically Loaded PSC Girders

Figure 3-19: Testing Setup Photo for Statically Loaded PSC Girders

3.5.3 PSC Girders Dynamically Loaded

The dynamically loaded girders were tested under a three point loading arrangement using a 100 kip MTS actuator at the FDOT structures research lab. The 20-ft long PSC girders spanned nineteen feet between the centerlines of the bearing pads which rested on stationary supports. The girder loading was applied by cycling between 25kips and 32kips at a frequency of 3 Hertz. Other than the load measurements recorded by the MTS actuator, the girders were also instrumented with four LVDT (linear variable differential transformer) deflection gages and up to eleven strain gages (30 mm long- 120 ohm). Two LVDT deflection gages were positioned at center span on each side of the girder and two LVDTs were placed at girder top surface above the support areas. On each girder, five of the strain gages were placed along the height of the cross-section at mid-span and the remaining strain gages were distributed along the flexural tension side at various locations depending on the CFRP

configuration. The general placements of all measurement devices mentioned are also shown in Figure 3-20 and a photo is available in Figure 3-21.

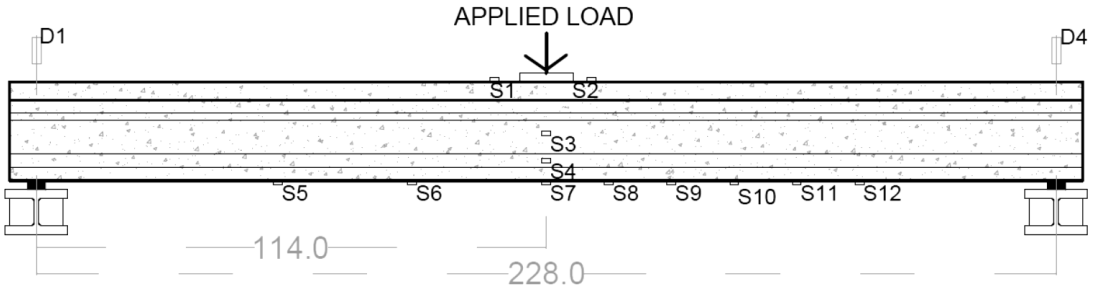

Figure 3-20. Testing Setup Schematic for Dynamically Loaded PSC Girders

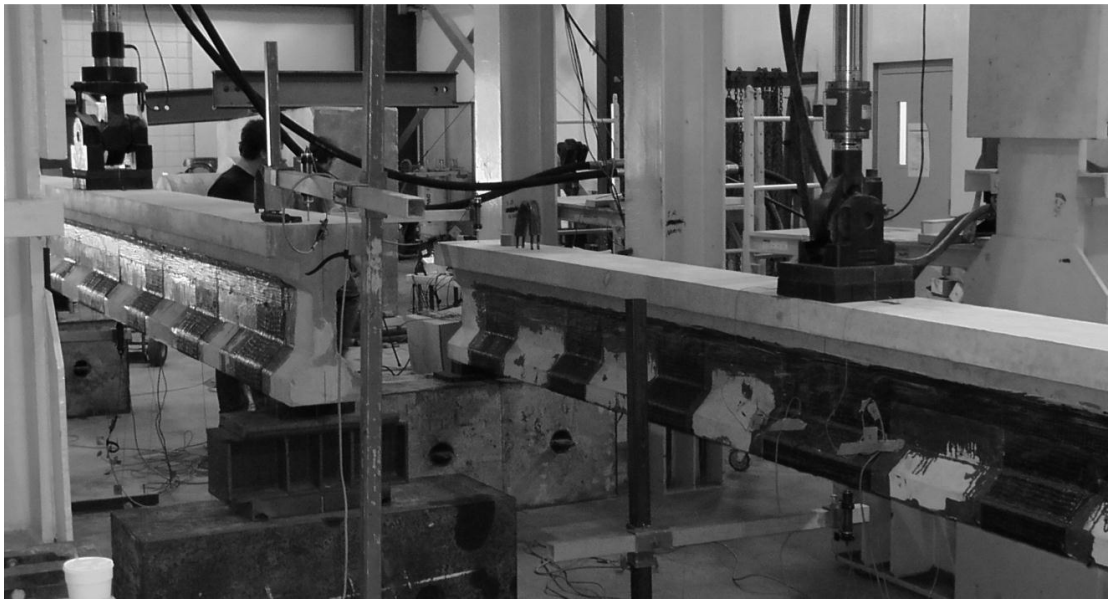

Figure 3-21: Testing Setup Schematic for Dynamically Loaded PSC Girders

CHAPTER 4:
EXPERIMENTAL FINDINGS

4.0 EXPERIMENTAL FINDINGS

This chapter presents the experimental data recorded from testing 34 RC beams and 13 PSC girders. The data of behavioral properties monitored and documented include the loading, deflections, strains, failure modes, and general observations.

4.1 SUMMARY OF DATA

Listed in the summary for each group of statically tested beams are values of the maximum loads, mid-span deflections at failure, tensile strains at beams' soffit, failure mode, and the enhancements percentages of moment capacity due to repairs. Observed behaviors at failure were recorded during each test and are also presented; though more technical lists of the failure modes are available within the results. The summary of the fatigue data is discussed more generally though load ranges, cycles, and deflection ranges are listed.

4.1.1 Steel Reinforcing Materials

First it is appropriate to report the findings of the material testing performed on the steel reinforcements used in the RC test specimens. This was executed to verify the properties of the reinforcements with intentions to get the exact values available to ensure the analytical evaluations were as accurate as possible. The design values

from the manufacturer and the values resulting from ASTM testing for all steel reinforcements used in the RC beams are presented in Tables 4-1 and 4-2.

Table 4-1: Test Results of Tensile Strengths for Steel Reinforcement

Rebar Tensile Specimens			Ultimate Load	Ultimate Tensile Stress
Specimen	Size	Area		
Design values	#3	0.11	6600	60000
Specimen 1	#3	0.11	7920	72000
Design values	#4	0.2	12000	60000
Specimen 2	#4	0.2	15090	75450

Table 4-2: Test Results of Tensile Strengths for RC Welded Wire Reinforcing Cage

1/16" Welded-Wire Frame Tensile Specimens			Ultimate Load	Ultimate Tensile Stress
Specimen	Wire Dia.	Area		
Design values	0.073	0.0042	252	60000
Specimen 1	0.073	0.0042	280	66899
Specimen 2	0.072	0.0041	275	67543
Specimen 3	0.073	0.0042	272	64988

4.1.2 RC Beams - Set #1 ("TB" set)

Load & Deflection: The maximum load and corresponding mid-span deflections for the first set of RC beams containing the #4 rebar are shown in Table 4-1. Also, presented in Table 4-1 are the percentages of maximum capacity gained from both the strengthened/repaired undamaged control beam and the repaired damaged control beam. The undamaged control beam is represented by the designation RC 1-1 and held a maximum load of 14.26kips, whereas the damaged control beam is represented by the designation RC 1-2 and only held a maximum load of 10.245kips. The remainder of the beams in this set received CFRP repair applications and have not only restored the lost capacity incurred from the imposed damage, but enhancements ranging from 10 to 48 percent are experienced by the repaired damaged beams with

bonded CFRP laminates. Detailed comparisons between the multiple various repair configurations are discussed in section 4.3 Presentation of Results.

Table 4-3: Max Load, Deflections, and Percent of Gained Capacity for 1st RC Set

Beam designation	max load (kip)	corresponding deflection (in.)	% gained from damaged beam	% gain from undamaged beam
RC 1-1	14.160	0.958	38%	0%*
RC 1-2	10.245	1.661	0%*	-28%**
RC 1-3	20.910	1.185	104%	48%
RC 1-4	16.450	0.914	61%	16%
RC 1-5	15.589	0.682	52%	10%
RC 1-6	16.654	0.864	63%	18%
RC 1-7	16.578	1.020	62%	17%
RC 1-8	18.710	0.904	83%	32%
RC 1-9	19.717	0.879	92%	39%
RC 1-10	17.122	0.843	67%	21%
RC 1-11	18.866	0.931	84%	33%
RC 1-12	19.641	1.050	92%	39%
RC 1-13	17.948	0.748	75%	27%
RC 1-14	18.407	0.860	80%	30%
RC 1-15	18.683	0.891	82%	32%

*Control beams compared to themselves render 0% increases
**Represents percentage lost from induced damage to beams

Table 4-4: Values of Max Micro-Strain of Beams' Soffit at Multiple Load Levels

Beam designation	Value of max strain in longitudinal CFRP at mid-span		
	@ 5 kips	**@ 10 kips**	**@ 15 kips**
RC 1-5	1017.7	2205.7	5464.3
RC 1-6	918.8	1857.7	5476.0
RC 1-7	322.2	1641.9	5946.4
RC 1-8	1221.0	2129.0	5005.5
RC 1-9	509.9	1941.3	4134.4
RC 1-10	626.4	2055.9	5579.5
RC 1-11	575.8	2020.8	4729.2
RC 1-12	268.9	1700.3	3882.9
RC 1-13	515.6	1939.6	5211.8
RC 1-14	279.7	1476.4	3792.4
RC 1-15	245.1	1763.4	3933.8

Max Tensile Strain: The maximum tensile strain experienced by the longitudinal CFRP laminates at the mid-span of the tested beams at multiple load levels is listed previously in Table 4-4.

Similarly, the percent of maximum strain decreased due to intermediate CFRP U-wrapping anchoring configurations at multiple load levels is shown in Table 4-5. The presented percents are calculated by comparing strains to those felt by RC 1-5 which utilized only end anchorage transverse U-wrappings and not intermediate anchors.

Table 4-5: Percent of Max Strain Decrease due to Intermediate Anchoring

Beam designation	% of max strain decreased due to intermediate anchoring		
	@ 5 kips	**@ 10 kips**	**@ 15 kips**
RC 1-5	0.0%*	0.0%*	0.0%*
RC 1-6	9.7%	15.8%	-0.2%
RC 1-7	68.3%	25.6%	-8.8%
RC 1-8	-20.0%	3.5%	8.4%
RC 1-9	49.9%	12.0%	24.3%
RC 1-10	38.4%	6.8%	-2.1%
RC 1-11	43.4%	8.4%	13.5%
RC 1-12	73.6%	22.9%	28.9%
RC 1-13	49.3%	12.1%	4.6%
RC 1-14	72.5%	33.1%	30.6%
RC 1-15	75.9%	20.1%	28.0%
*Control repair configuration compared to themselves renders 0% increases			

Observed Failure Mode Behaviors: During the flexural testing of the fifteen RC beams in this first set, observations of behaviors at the moments just prior to failure were noted. These descriptions of failure provide first hand observational data of what was seen during failure. To note, the observations at failure presented in Table 4-6 are only visual evidence which was documented during testing. The technical failure modes for each specimen were verified through the measured and recorded

data from testing and are available in a following section of this paper (section 4.3 Presentation of Results).

Table 4-6: Observed Behaviors during Testing at Failure

Beam	Observations at Failure
RC 1-1	excessive flexural cracks and crack widening
RC 1-2	compression failure with slight delamination
RC 1-3	excessive flexural cracks and crack widening
RC 1-4	debonding failure of entire right side of CFRP
RC 1-5	delamination of CFRP with concrete attached
RC 1-6	slight debonding instantly followed by rupture
RC 1-7	slight debonding instantly followed by rupture
RC 1-8	slight debonding instantly followed by rupture
RC 1-9	CFRP rupture
RC 1-10	CFRP rupture
RC 1-11	slight compression cracking then rupture
RC 1-12	CFRP rupture
RC 1-13	slight compression cracking then rupture
RC 1-14	slight debonding on one side instantly followed by rupture
RC 1-15	compression failure w/ splitting of center U-wrap

4.1.3 RC Beams - Set #2 ("JB" set)

Load & Deflection: The maximum load and corresponding mid-span deflections for the second set of RC beams containing the #3 rebar are shown in Table 4-5. Also, presented in Table 4-7 are the percentages of maximum capacity gained from both the strengthened/repaired undamaged control beam and the repaired damaged control beam. RC 2-1 represented the virgin beam having no imposed damage and no CFRP repair with a recorded maximum capacity of 9.31 kips.; whereas RC 2-2 represented the lower bound of the set having simulated imposed damage but no CFRP repair and it experienced a maximum load capacity of only 7.14 kips. The difference of these

two control beams yields a twenty-three percent loss in ultimate carrying capacity associated to the imposed simulated damage.

Table 4-7: Max Load, Deflections, and Percent of Gained Capacity for 2nd RC Set

Beam designation	max load (kip)	corresponding deflection (in.)	% gained from damaged beam	% gain from undamaged beam
RC 2-1	9.310	2.350	30%	0%*
RC 2-2	7.141	0.699	0%*	-23%**
RC 2-3	15.215	0.401	113%	63%
RC 2-4	14.327	0.357	101%	54%
RC 2-5	21.216	0.630	197%	128%
RC 2-6	22.813	0.671	219%	145%
RC 2-7	16.840	0.554	136%	81%
RC 2-8	26.879	1.160	276%	189%
RC 2-9	27.248	1.546	282%	193%
RC 2-10	22.907	0.686	221%	146%
RC 2-11	32.366	1.068	353%	248%
RC 2-12	31.987	0.923	348%	244%
RC 2-13	27.758	0.923	289%	198%
RC 2-14	18.007	0.958	152%	93%
RC 2-15	24.549	0.487	244%	164%
RC 2-16	23.818	0.859	234%	156%
RC 2-17	23.266	0.694	226%	150%
RC 2-18	21.613	0.710	203%	132%
RC 2-19	22.321	0.825	213%	140%

*Control beams compared to themselves render 0% increases
**Represents percentage lost from induced damage to beams

The beams in this set that received CFRP repair applications have not only restored the lost capacity incurred from the imposed damage, but enhancements ranging from 54 to 248 percent are experienced; with the highest capacity reaching up to 32.366kips.

Max Tensile Strain: The maximum tensile strains developed at mid-span of the beams soffit felt by the longitudinal CFRP laminate at multiple load levels is listed in Table 4-8. Likewise, the percentage of decreased strain due to intermediate

transverse anchors is provided in Table 4-9. To note, excessively large values may indicate broken strain gages; details of these aspects are discussed in detail in section 4.3 (Presentation of Results).

Table 4-8: Values of Max Strain of Beams' Soffit at Multiple Load Levels

Beam designation	Value of max strain in longitudinal CFRP at mid-span		
	@ 5 kips	@ 10 kips	@ 15 kips
RC 2-5	415.0	1434.5	2651.3
RC 2-6	569.7	1636.3	2877.3
RC 2-7	768.3	2106.6	22793.7
RC 2-8	443.1	1459.5	3017.9
RC 2-9	440.6	1505.2	2662.7
RC 2-10	502.6	1494.3	2940.3
RC 2-11	381.5	1390.5	2461.6
RC 2-12	462.6	1443.1	2458.2
RC 2-13	714.8	1671.8	3247.7
RC 2-14	471.1	1412.1	2495.1
RC 2-15	N/A	N/A	N/A
RC 2-16	234.1	1400.5	2762.1
RC 2-17	231.9	1403.3	2510.3
RC 2-18	540.5	1536.7	2902.3
RC 2-19	643.7	1742.5	3226.1

Table 4-9. Percent of Max Strain Decreased due to Intermediate Anchoring

Beam designation	% of max strain decreased due to intermediate anchoring		
	@ 5 kips	**@ 10 kips**	**@ 15 kips**
RC 2-5	35.5%	17.7%	17.8%
RC 2-6	11.5%	6.1%	10.8%
RC 2-7	N/A	N/A	N/A
RC 2-8	31.2%	16.2%	6.5%
RC 2-9	31.5%	13.6%	17.5%
RC 2-10	21.9%	14.2%	8.9%
RC 2-11	40.7%	20.2%	23.7%
RC 2-12	28.1%	17.2%	23.8%
RC 2-13	-11.0%	4.1%	-0.7%
RC 2-14	26.8%	19.0%	22.7%
RC 2-15	N/A	N/A	N/A
RC 2-16	63.6%	19.6%	14.4%
RC 2-17	64.0%	19.5%	22.2%
RC 2-18	16.0%	11.8%	10.0%
RC 2-19	0.0%*	0.0%*	0.0%*
*Control repair configuration compared to themselves render 0% increases			

Observed Failure Mode Behaviors: The observations at beam failure presented in Table 4-10 are only visual evidence which was documented during testing, the technical failure modes for each specimen are available in a following section of this thesis (section 4.3 Presentation of Results).

Table 4-10. Observed Behaviors during Testing at Failure

Beam	Observations at Failure
RC 2-1	excessive flexural cracks and crack widening
RC 2-2	excessive flexural cracks and crack widening
RC 2-3	debonding from one side of CFRP
RC 2-4	debonding from one side of CFRP
RC 2-5	debonding from one side after excessive cracking
RC 2-6	shear failure
RC 2-7	CFRP rupture (beam only had 1 layer of CFRP)
RC 2-8	slight debonding then compression failure
RC 2-9	excessive shear cracking then compression failure
RC 2-10	excessive shear cracking then compression failure
RC 2-11	shear failure
RC 2-12	CFRP rupture at mid-span
RC 2-13	CFRP rupture w/ zipper type failure
RC 2-14	shear failure
RC 2-15	shear failure
RC 2-16	shear failure
RC 2-17	shear failure
RC 2-18	shear failure
RC 2-19	excessive flexural cracking then debonding failure

4.1.4 Statically Loaded PSC Girders

Load & Deflection: The maximum load and corresponding mid-span deflections for the ten statically tested PSC girders are shown in Table 4-9. Also, presented in Table 4-11 are the percentages of maximum capacity gained from both the undamaged control beam and the damaged control beam. The undamaged control beam is represented by the designation PS-1 which held a maximum load of 75.87kips, whereas the damaged control beam is represented by the designation PS-2 and only held a maximum load of 61.88kips. The remaining girders received CFRP repair applications and not only restored the lost capacity incurred, but experienced enhancements ranging from 2 to 38 percent.

Table 4-11: Max Load, Deflections, and Percentages of Gained Capacity for PSC Set

Beam designation	Max Load (kips)	Corresponding deflection (in.)	% increase from damaged beam	% increase from undamaged beam
PS-1	75.87	6.94	23%	0%*
PS-2	61.88	5.38	0%*	-18%**
PS-3	90.14	2.44	46%	19%
PS-4	84.75	2.14	37%	12%
PS-5	78.92	1.61	28%	4%
PS-6	100.91	2.39	63%	33%
PS-7	104.42	2.74	69%	38%
PS-8	99.16	2.29	60%	31%
PS-9	77.26	1.58	25%	2%
PS-10	87.68	2.15	42%	16%

*Control beams compared to themselves render 0% increases
**Represents percentage lost from induced damage to beams

Max Tensile Strain: The maximum tensile strains of the PSC girders are listed in Table 4-12.

Table 4-12: Values of Max Strain of Beams' Soffit at Multiple Load Levels

Beam Designation	**Maximum Strain Values Recorded at Various Loads**					
	@ 5 kip	@ 15 kip	@25 kip	@ 40 kip	@ 60 kip	@ 70 kip
PS-1	52.58	158.51	280.33	291.40*	broke	broke
PS-2	61.32	200.39	1837.30	broke	broke	broke
PS-3	51.03	167.19	314.76	1295.52	2984.16	4075.28
PS-4	55.16	172.14	341.49	1332.85	3197.49	4146.04
PS-5	53.03	146.52	316.97	1270.22	5213.27	8939.73
PS-6	51.57	160.54	292.03	1048.55	2646.34	3393.13
PS-7	49.05	150.30	266.07	835.90	2415.59	3203.85
PS-8	52.59	161.94	281.84	942.62	2647.17	3616.50
PS-9	58.40	180.76	368.50	1357.88	3433.54	5409.16

* Strain gages have been determined unreliable; & green equals lowest value recorded at that load

Observed Failure Mode Behaviors: The observations at beam failure are presented in Table 4-13, and are only visual evidence which was documented during testing.

Table 4-13: Observed Behaviors during Testing at Failure

Beam Designation	**Failure Mode and Observations of Behavior during Testing**
PS-1	flexural failure started with visible widening of flexural cracks around 60 kips, cracks widen to an estimated eighth of an inch at 68 kips, ultimately compression failure caused the beam to completely fail around 76 kips
PS-2	flexural failure started with visible widening of flexural cracks around 35 kips, cracks widen excessively around 49 kips, ultimately a large compression/shear crack from flexural side up to load @ 25" off center
PS-3	debonding sound heard around 86 kips, CFRP rupture ultimately occurred at approx. 5 inches off center on the side of debonding/delamination, debonding spanned from about center of the beam to center of second u-wrap span
PS-4	debonding sounds heard around 80 kips, CFRP rupture ultimately occurred at approx. 7 or 8" inches off center on the side of debonding/delamination, debonding spanned from point of rupture to center of second u-wrap span
PS-5	debonding sounds heard around 75 kips, CFRP rupture ultimately occurred at center span, debonding/delamination spanned from just pasted fist u-wrap on one side to beginning of first on the other side
PS-6	debonding sounds heard around 95 kips, CFRP debonding/delamination spanned from just pasted center u-wrap to beginning of last u-wrap, the first u-wrap was also completely debonded-originating from top of wrap
PS-7	Load reached 105 then dropped to 95 before failure, CFRP debonding/delamination spanned from just pasted center u-wrap to end of last u-wrap, the second u-wrap was also completely debonded-originating from top of wrap
PS-8	debonding sounds heard around 95 kips, CFRP rupture ultimately occurred at center, two local debonding areas formed-one occurred in first u-wrap span on one side, the other was from first wrap to last wrap on the opposite side
PS-9	localized debonding of center u-wraps at top of beam and perhaps other debonding sounds heard around 75 kips, ultimately CFRP rupture at center span, debonding/ delamination did occur in center section approx. 60" total

4.1.5 Dynamically Loaded PSC Girders

The loading sequence of the girders began by increasing the applied load up to a load level slightly higher than the cracking load to simulate a typical overloading condition. The girder was then unloaded, and reloaded again at a rate of 2.5 mm/min (0.1 in. /min) to measure the load corresponding to opening of the flexural cracks. This loading sequence was selected to determine the effective prestressing force in the girders. For the given measured load at reopening of the flexural crack at mid-span, *P*ro, the average effective prestressing force in each strand, P_{eff}, was determined using the following equation:

The fatigue load range of 10 to 35 kips was used for testing the girders was designed to simulate typical loading of an actual bridge under the effect of the increased service loading conditions. The sinusoidal fatigue load was applied at a frequency of 2 Hz, and stopped periodically to conduct static loading tests to measure degradation. The range varies from a minimum load equivalent to the dead load and a maximum load equivalent to the combined dead and increased live load. For the test girders, the minimum load, in addition to the girder's own weight, included a load producing a moment equivalent to the moment due to an asphalt wearing surface, typically, used for these types of bridges. Assuming a wearing surface thickness of 102 mm (4 in.), a deck width of 775 mm (30.5 in.) and density of 23.56 kN/m^3 (150 lb/ft^3), an equivalent concentrated load representing the dead load acting at mid-span was calculated as 8.9 kN (2 k). The service load was determined based on a truck configuration specified by AASHTO HS-20 type loading. The axle load of 106.8 kN (24 k) was multiplied by the impact factor and the distribution factor according to AASHTO. The impact factor used was 1.33 as specified by AASHTO Article 3.6.2.1. The load distribution factor was determined from Table 4.6.2.2.2b-1 of the AASHTO specifications. Based on a two-lane bridge 9.30 m (30.5 ft) wide supported by 12 C-Channel girders, the distribution factor used was 0.24. Based on the maximum moment induced on the girder by the moving truck loads along the girder span of 9.14 m (30 ft), the equivalent concentrated load at mid-span was determined to be 40 kN (9.0 k). It should be mentioned that some of the original drawings for these girders indicated that for the longer span of 9.14 m _30 ft_, the specified load was HS-13 type loading, which is 13.3% less than the loading used in this investigation.

4.2 METHOD OF ANALYSIS

The primary methods of analysis used to direct the more efficient CFRP repair design is analyzed through comparing and contrasting the various behavior results from the experimental measurements recorded from each individual testing. The measurements included in these comparisons address the capacity of each beam, the measured deflections, stresses, strains, and the experienced failure modes.

4.3 PRESENTATION OF RESULTS

4.3.1 Reinforced Concrete Results

Reinforced Concrete Load/Deflection Results: Figure 4-1, shows a load deflection graph including the four tested beams which experienced the largest maximum load capacity compared with the two control beams. The control beams being 1-1, an undamaged beam and 1-2, a damaged beam with only a simulated concrete repair. It can be seen in this figure that the repaired beams maintained approximately the same stiffness but experienced a less ductile behavior and a large increase in capacity when compared to the control beams.

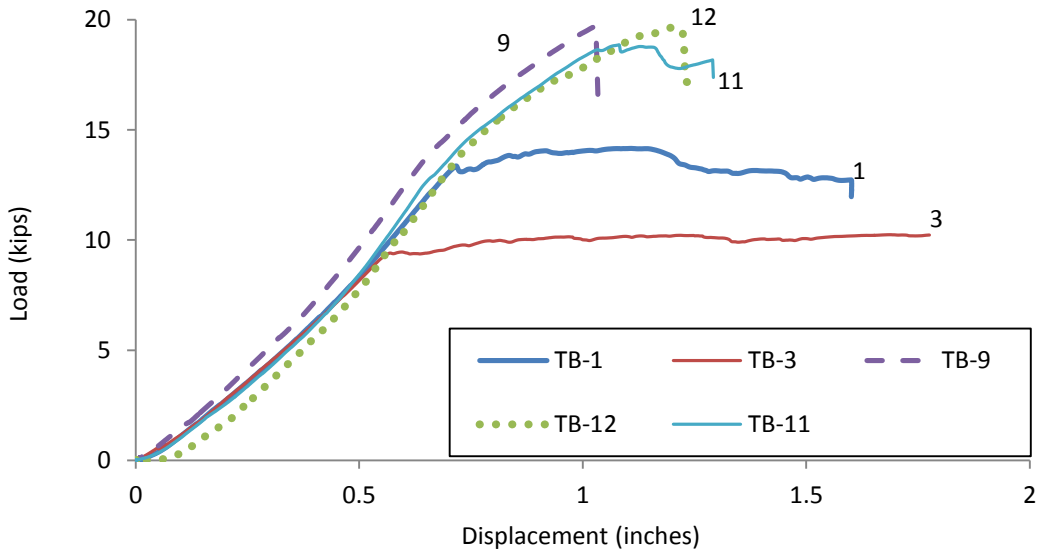

Figure 4-1: Load-deflection comparison of best performing repairs and control beams of 1st set ("TB" set)

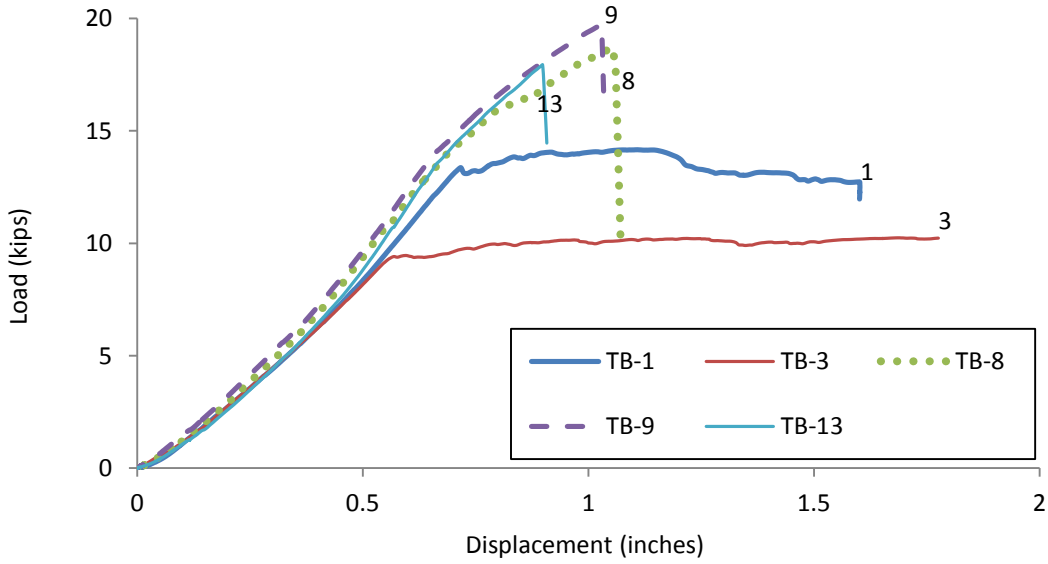

Figure 4-2: Load-deflection comparison of some repaired and control beams of 1st set ("TB" set)

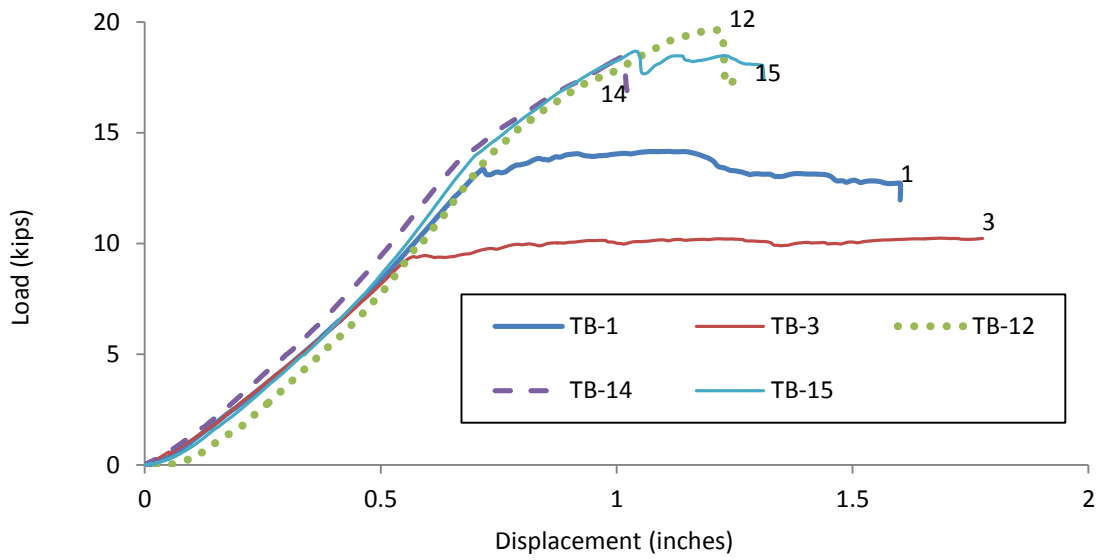

Figure 4-3: Load-deflection comparison of similar beams and control beams of 1st set

Figure 19 shows a load vs. deflection graph of the top performing repairs for the 2nd set compared to the control beams from its set.

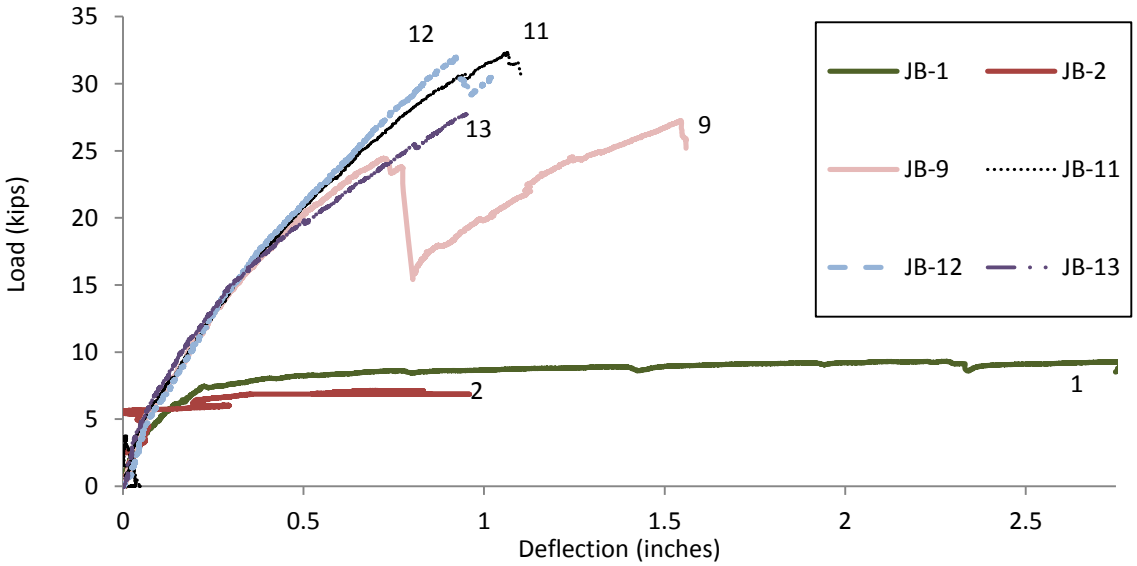

Figure 4-4: Load-deflection comparison of best repairs and control beams for 2nd set

A comparison between the failure load of damaged beam 2-2 (control damaged beam with no CFRP) and CFRP repaired beams 2-3 to 2-19 shows that the CFRP repair

enhanced the flexural capacity by a range of 101% to 353%. Also, increases in the failure load of 54% to 193% were observed for the CFRP repaired pre-damaged beams 2-3 to 2-19 when compared to an undamaged control beam (2-1).

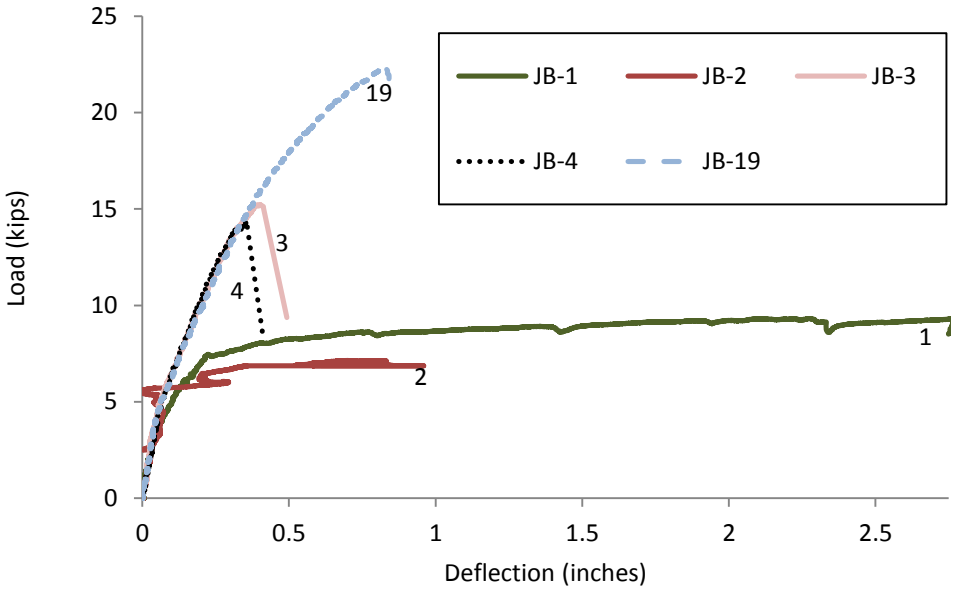

Figure 4-5: Load-deflection comparison concerning end anchorage

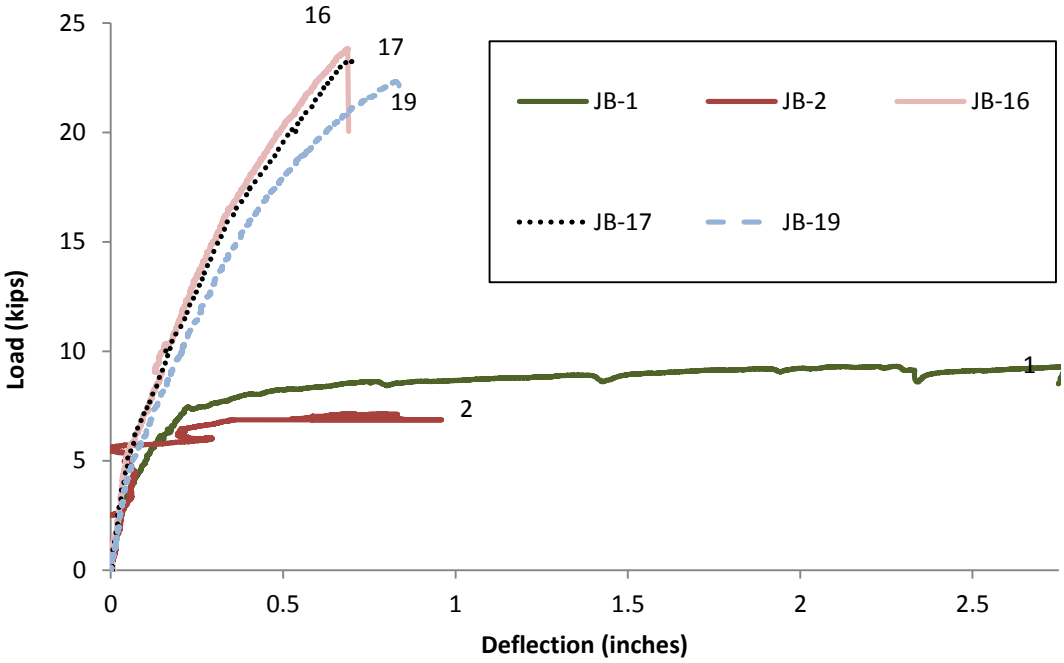

Figure 4-6: Load-deflection comparison concerning intermediate anchors

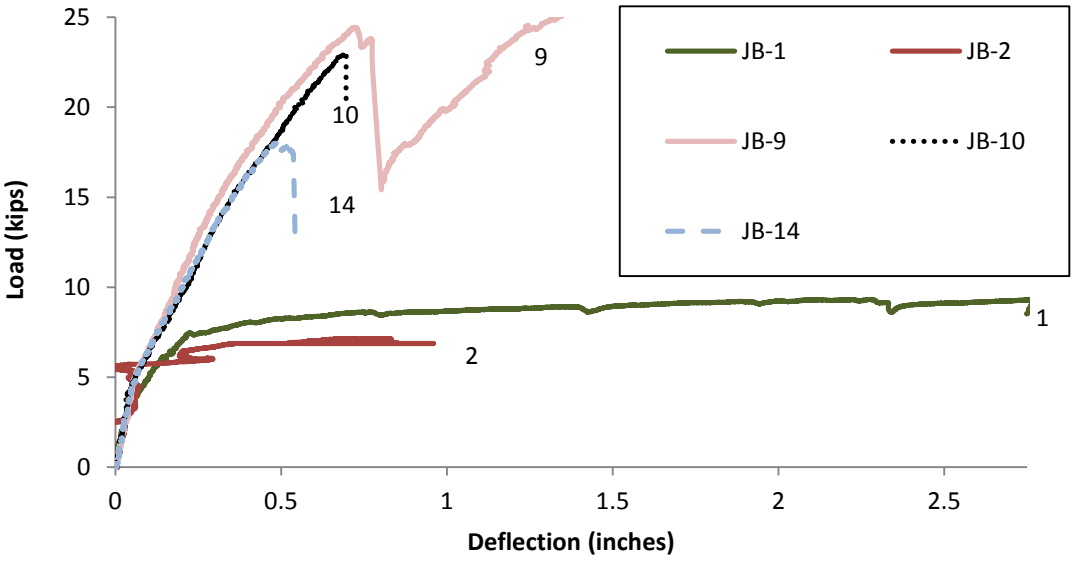

Figure 4-7: Load-deflection comparison concerning longitudinal length

Reinforced Concrete Strain Development Results: The comparison mentioned is graphically presented in Figure 23. It can be seen by the comparison in Figure 23 that the use of intermediate U-wraps for anchoring does suppress the strain developed in the longitudinal laminate applied to the beams soffit.

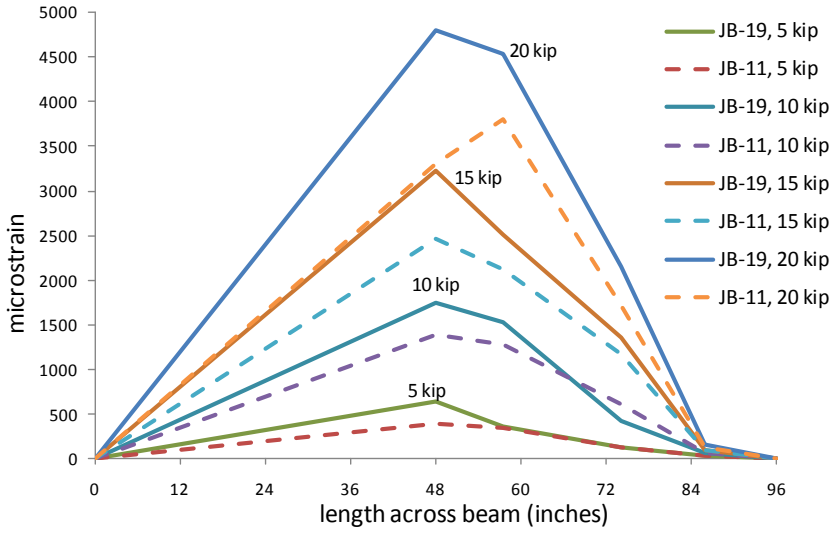

Figure 4-8: Comparison of strain developed along beams soffit for best repair and control beams from 2nd set ("JB" set)

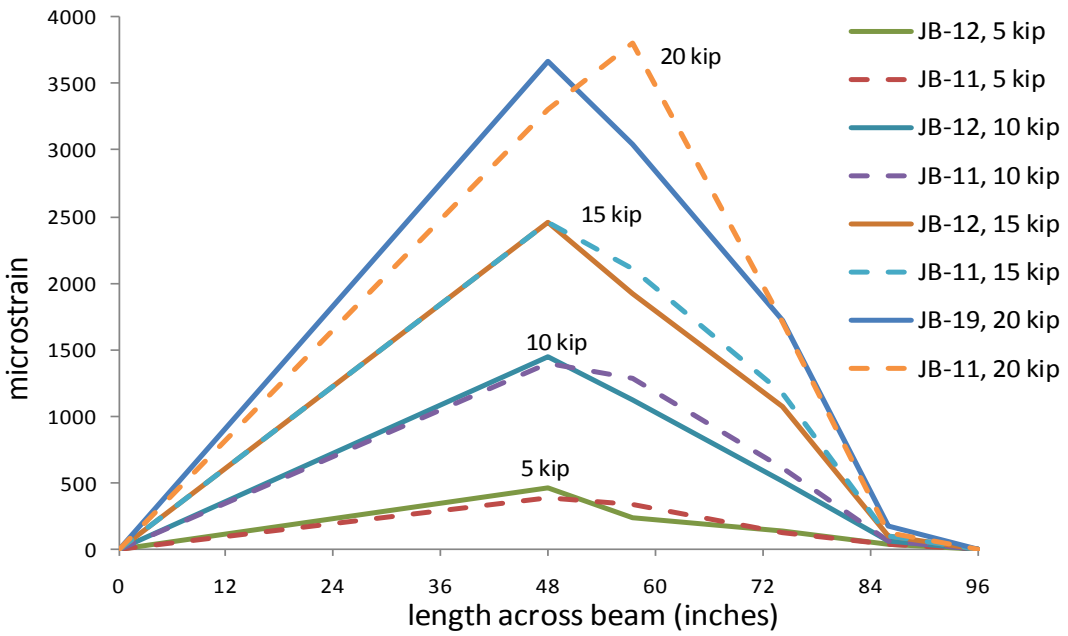

Figure 4-9: Comparison of strain developed along beams soffit for best repair and fully wrapped beam in 2nd set ("JB" set)

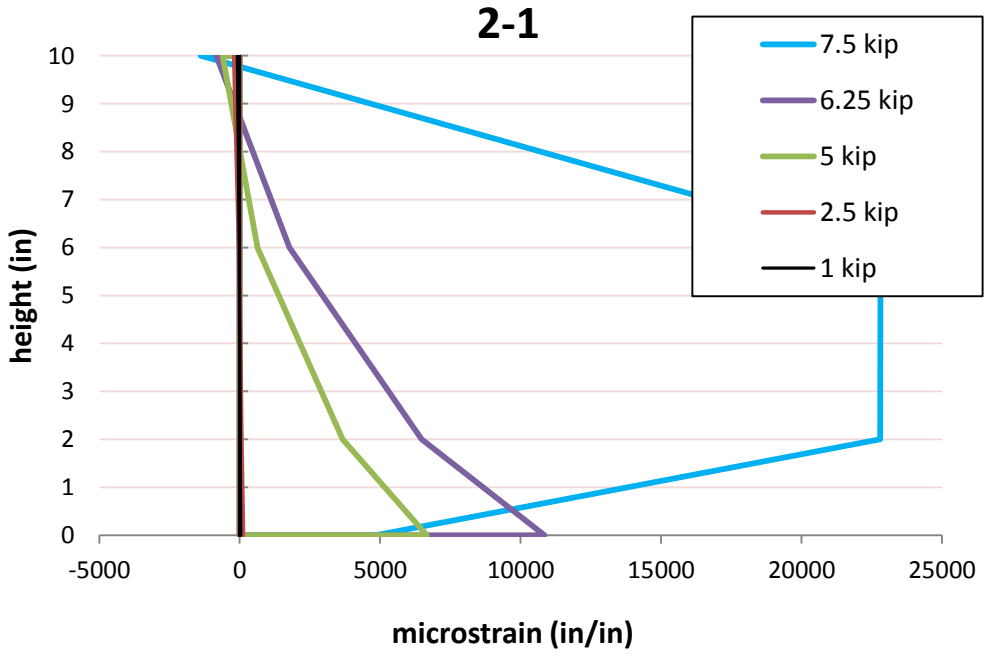

Figure 4-10: Strain per height of cross-section for Control beam of 2nd set at various loads

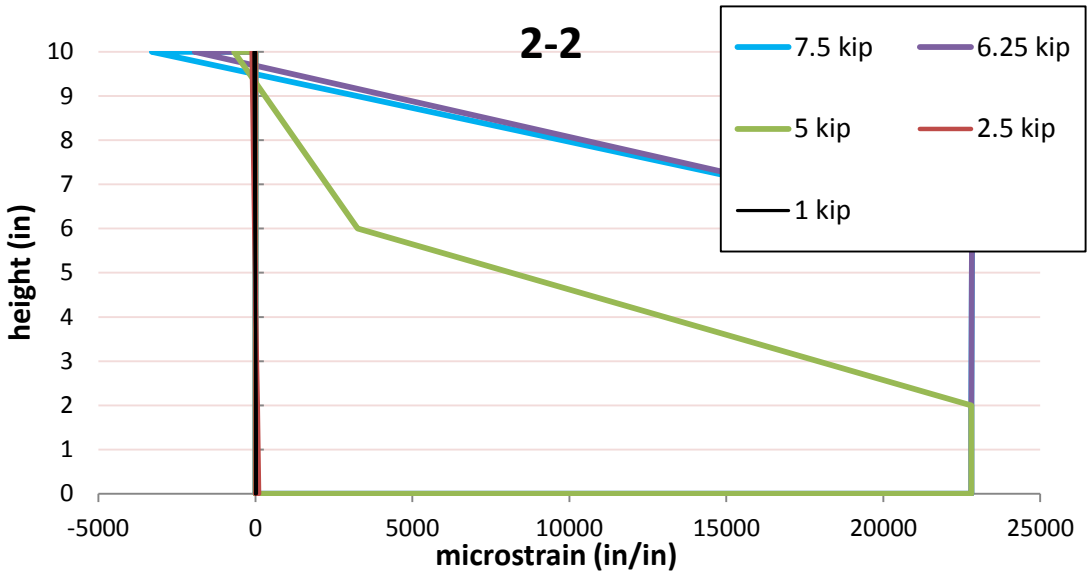

Figure 4-11: Strain per height of cross-section for Control beam of 2nd set ("JB" set) at various loads

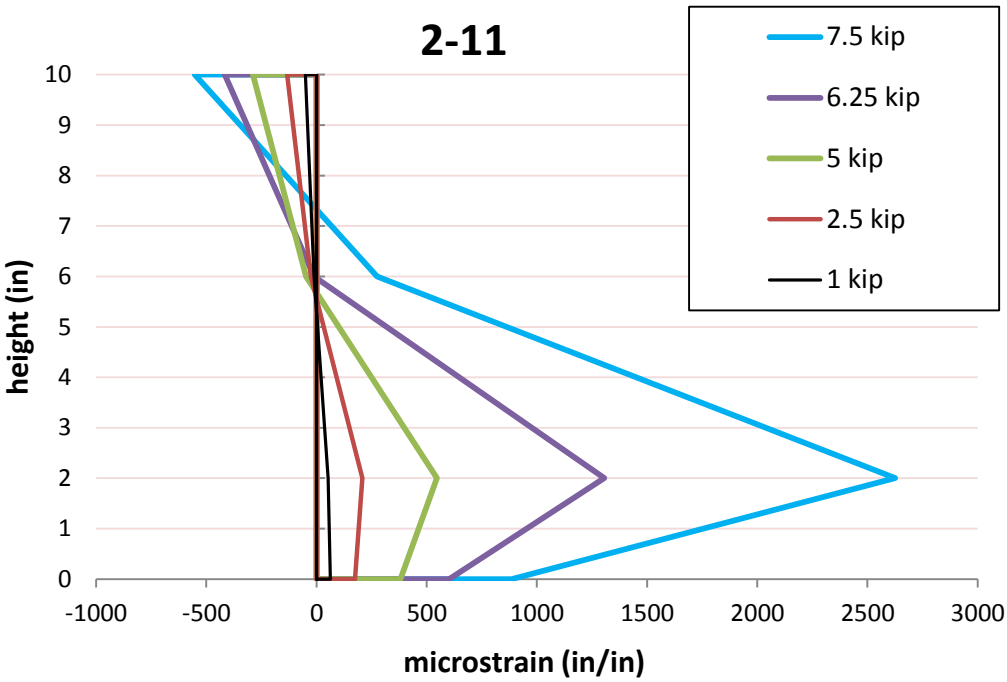

Figure 4-12: Strain per height of cross-section for repaired beam of 2nd set ("JB" set) at various loads

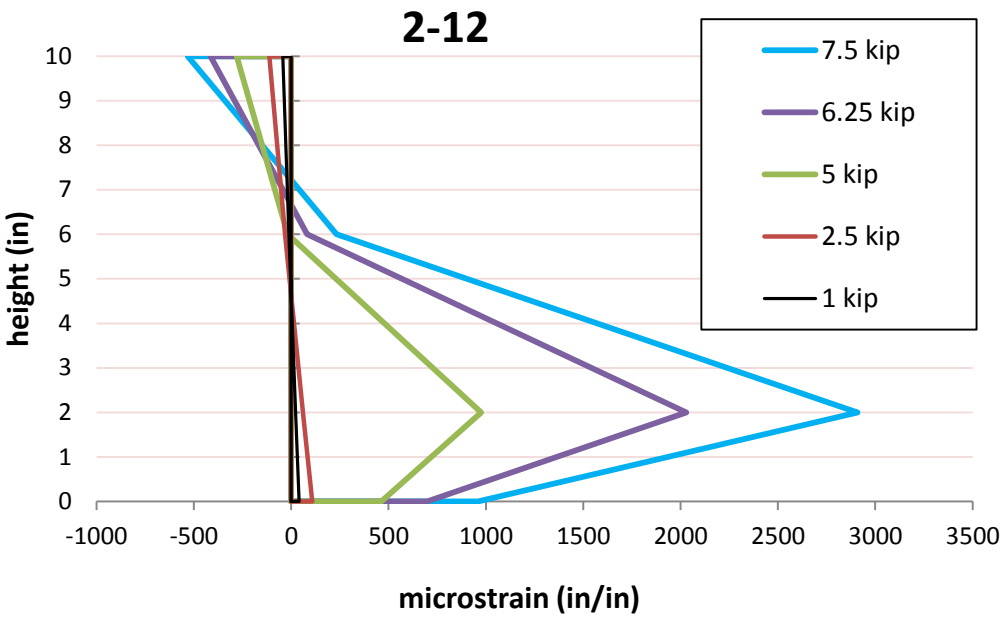

Figure 4-13: Strain per height of cross-section for repaired beam of 2nd set ("JB" set) at various loads

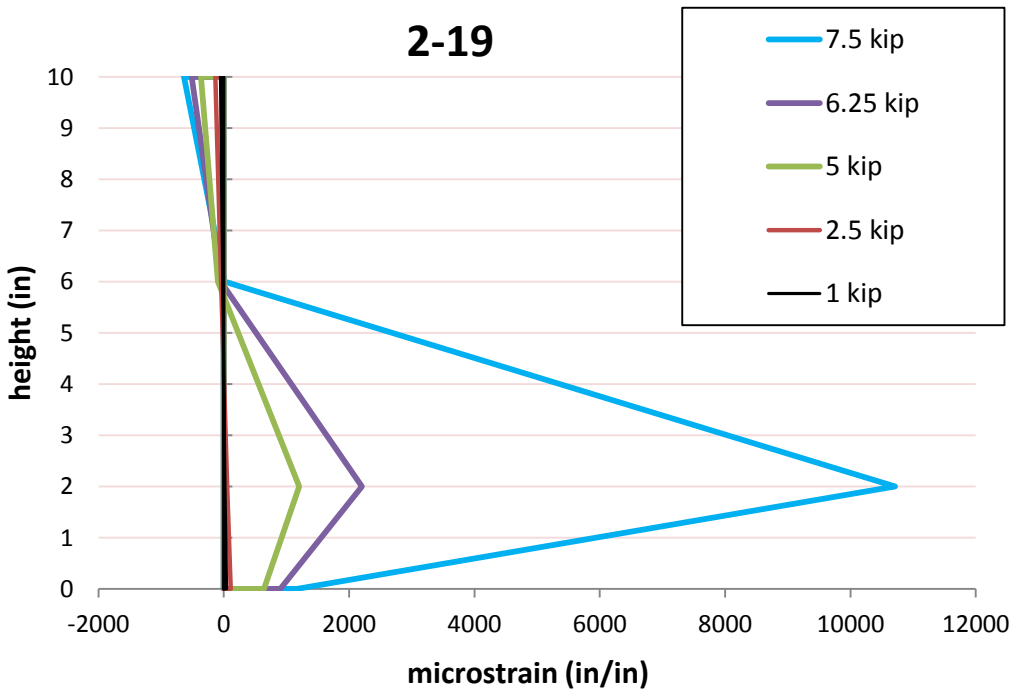

Figure 4-14: Strain per height of cross-section for repaired beam of 2nd set ("JB" set) at various loads

4.3.2 Half-Scaled Prestressed Results

Half-Scaled Load/Deflection Results: The graphical depiction of the load deflection results for each girder tested are presented in various comparisons in Figure 19 through Fig. 23.

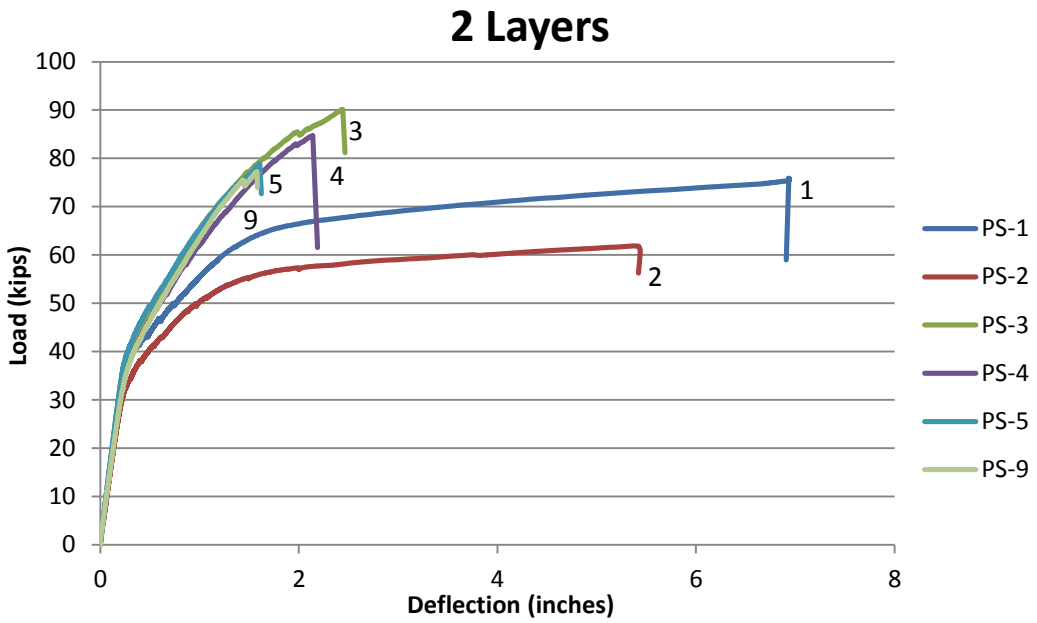

Fig. 4-15: Load vs. deflection for controls and girders with 2 layers of CFRP

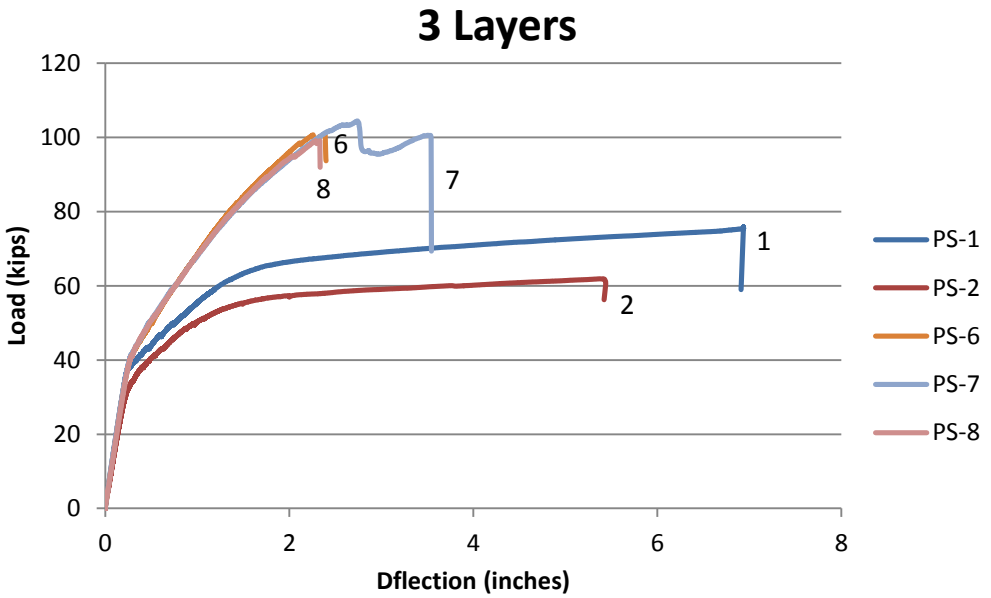

Fig. 4-16: Load vs. deflection for controls and girders with 3 layers of CFRP

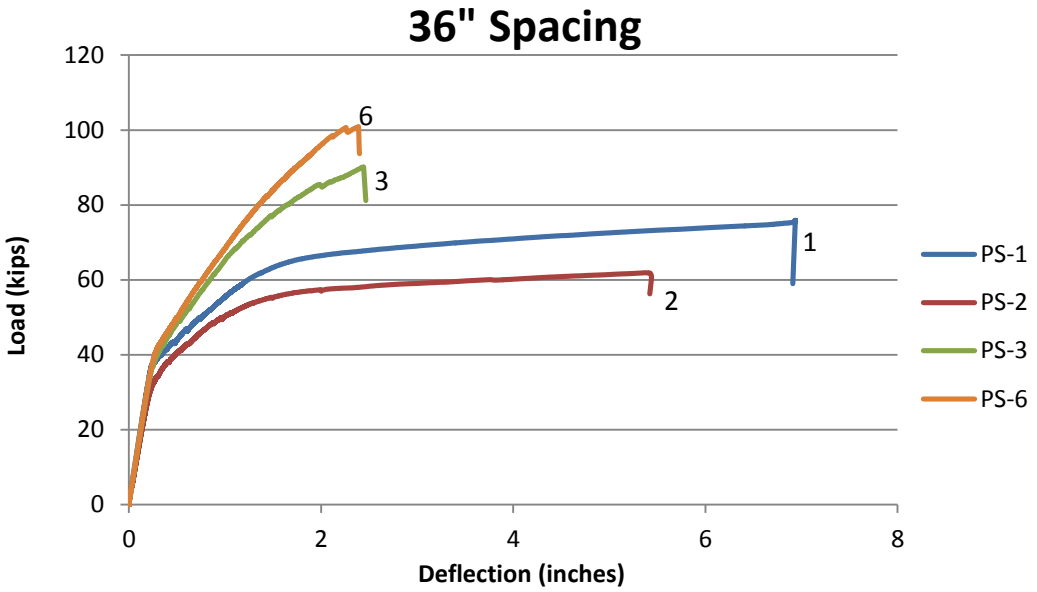

Fig. 4-17: Load vs. deflection for controls and 36" spacing configurations

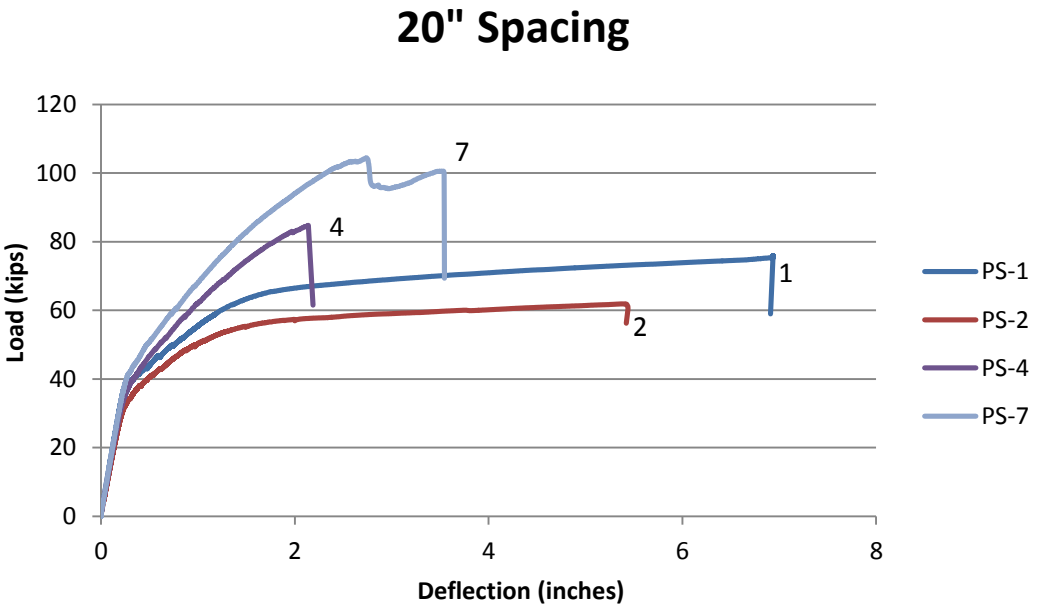

Fig. 4-18: Load vs. deflection for controls and 20" spacing configurations

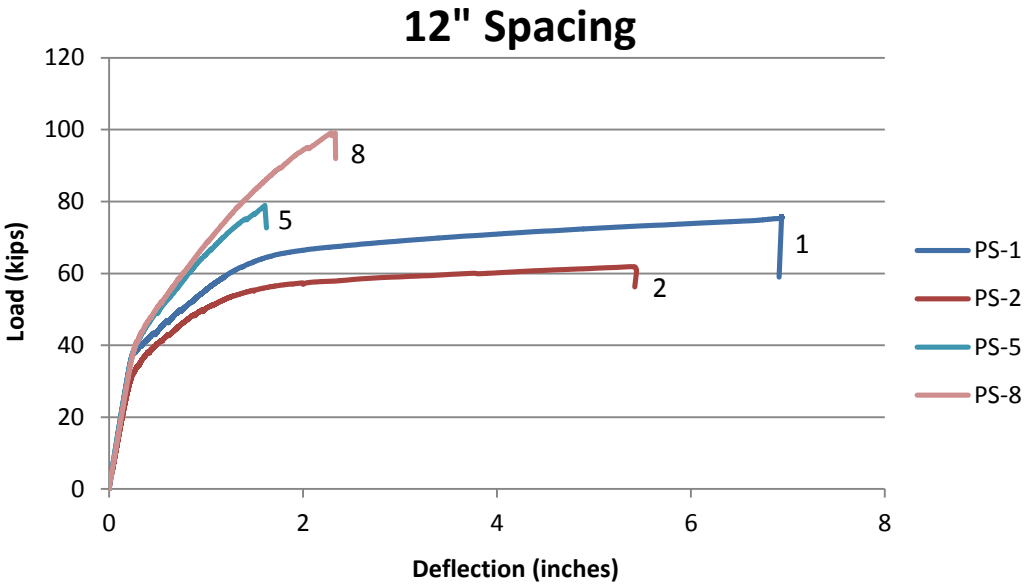

Fig. 4-19: Load vs. deflection for controls and 12" spacing configurations

As seen by the results, the damage and cutting of one of the prestressing strands (Girder PS-2) resulted in 18.44% loss in flexural capacity compared to the undamaged control girder PS-1. The CFRP repair of the damaged girder PS-2 as shown in girders PS3 to PS9 restored the damaged girder's capacity and exceeded the capacity of the undamaged control girder PS-1 by up to 37.63%. The results also show that U-shaped wrapping of CFRP laminates (Girders PS-3 to PS-8) enhanced the flexural capacity even if the U-wrapping was not continuously covering the entire girder side (not fully wrapped).

The strains measured at a load level of 70 kips are presented in Fig. 12. Half of the span lengths of the symmetrical girders were instrumented with a multitude of strain gages while the other half of the span length had one strain gage. Therefore, the profiles shown in Fig. 12 depict much more detailed behavior on the girder right side of the center peaks.

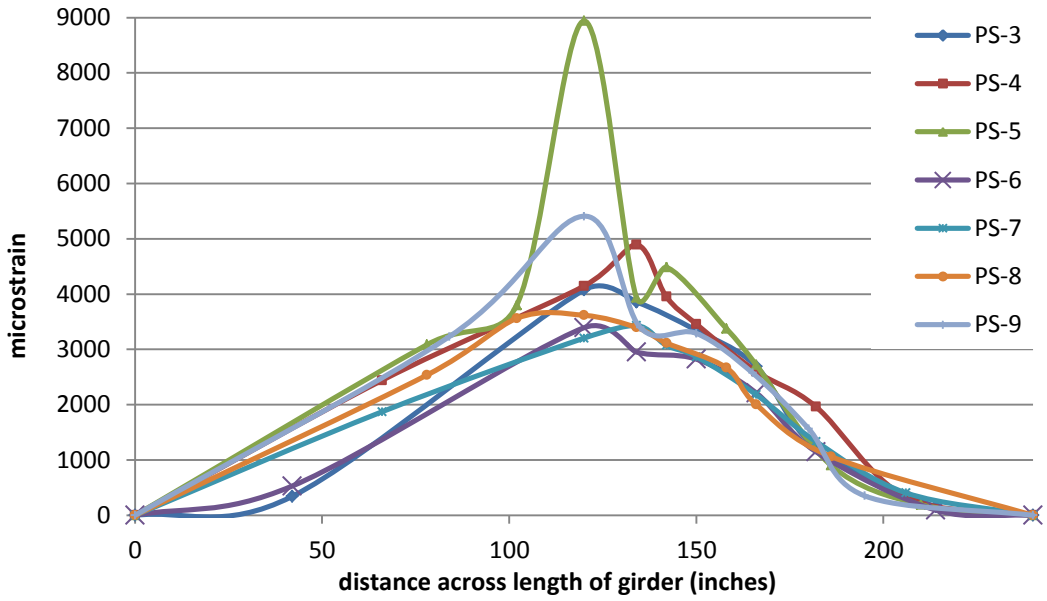

Fig. 4-20: Strain of CFRP at girder soffit vs. length for repaired girders

Half-Scaled Fatigue Testing Results: That the loading was designed to examine the behavior at a significantly higher fatigue load range. Premature degradation and failure of the repaired girders were noticed at the high load level range of fatigue. The beams failed after or around 500,000 cycles. Another set of beams is being tested with a normal fatigue load level. The graphical depiction of the load deflection results for each girder tested in fatigue are presented in Figures 36 thru 38.

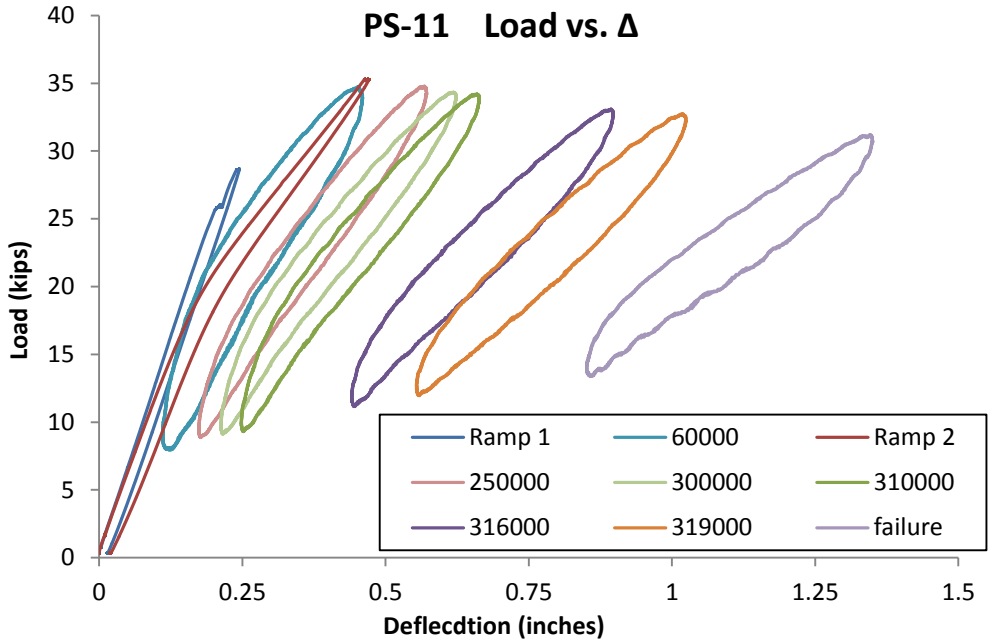

Figure 4-21: Fatigue Behavior and Degradation until Failure for Girder PS-11

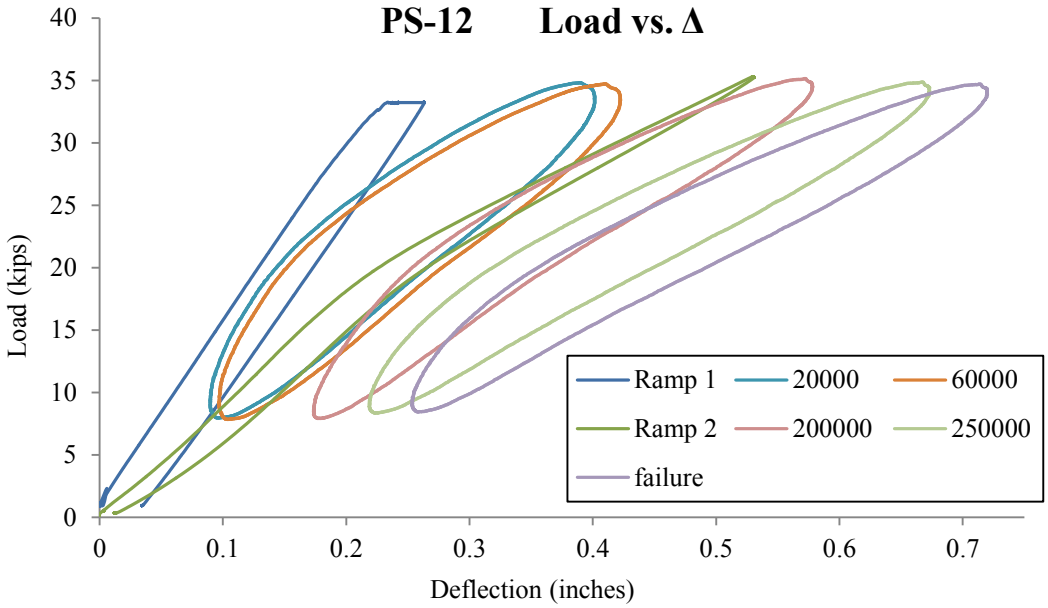

Figure 4-22: Fatigue Behavior and Degradation until Failure for Girder PS-12

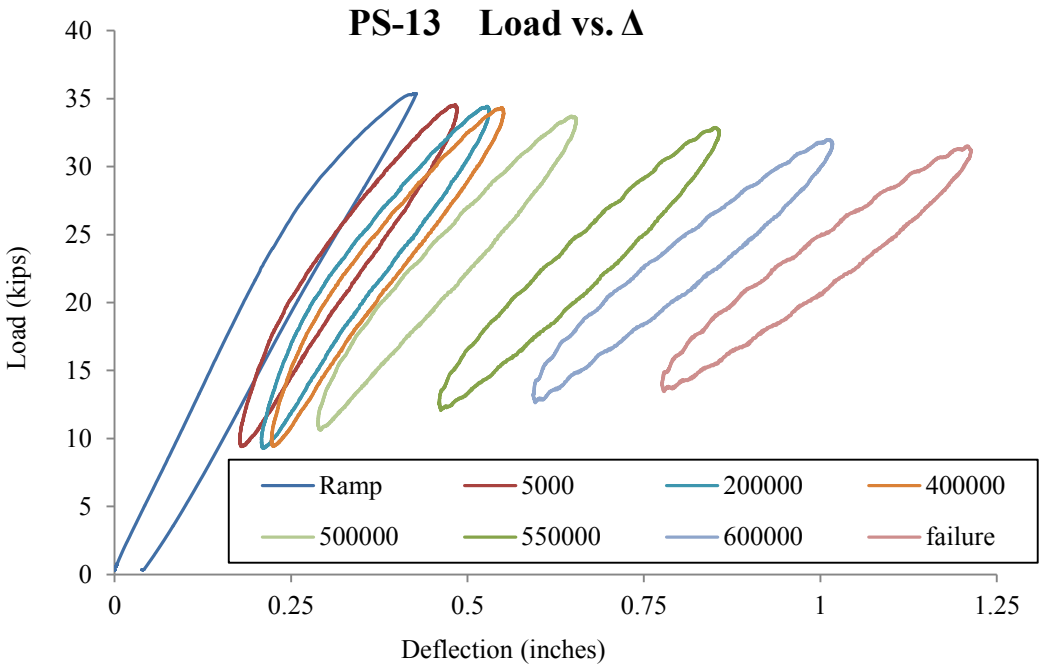

Figure 4-23: Fatigue Behavior and Degradation until Failure for Girder PS-13

CHAPTER 5
ANALYTICAL FINDINGS

5.1 SUMMARY OF ANALYTICAL DATA

RC Beams: Tables 5-1 & 5-2 list the percentages of increased or decreased deflections and loads compared to the calculated predictions; documenting the percent difference between the models and actual values. The load chosen for evaluation of this stage was 18.18kip (80.87N) for the first set and 22.67kip (100.84N). These load values rendered deflection and curvature values of 0.675in (17.15mm) and $8.7E^{-4}$rad for the first set and values of .846in (21.49mm) and $1.1E^{-3}$rad for the second set.

Table 5-1: Percent increased or decreased from predicted Capacity Values (set 1)

Percents increased or decreased from predicted values		
Beam designation	**LOADS:** predicted = 18.18 kip	**DEFLECTIONS:** predicted: 0.675 in.
TB-5	14.25%	1.01%
TB-6	8.39%	28.02%
TB-7	8.81%	51.17%
TB-8	2.92%	33.98%
TB-9	8.45%	30.28%
TB-10	5.82%	24.84%
TB-11	3.77%	37.97%
TB-12	8.04%	55.60%
TB-13	1.27%	10.86%
TB-14	1.25%	27.46%
TB-15	2.77%	32.00%

Table 5-2: Percent increased or decreased from predicted Capacity Values (set 2)

Percents increased or decreased from predicted values		
Beam designation	**LOADS:** predicted = 22.67 kip	**DEFLECTIONS:** predicted: 0.846 in.
RC 2-5	6.41%	25.50%
RC 2-6	0.63%	20.66%
RC 2-7	25.72%	34.56%
RC 2-8	18.56%	37.11%
RC 2-9	20.19%	82.71%
RC 2-10	1.04%	18.86%
RC 2-11	42.77%	26.26%
RC 2-12	41.10%	9.09%
RC 2-13	22.44%	9.09%
RC 2-14	20.57%	13.25%
RC 2-15	8.29%	42.38%
RC 2-16	5.07%	1.59%
RC 2-17	2.63%	18.00%
RC 2-18	4.66%	16.07%
RC 2-19	1.54%	2.49%

PSC Girders: There was a considerably noticeable discrepancy between the predicted capacity predictions and the actual measured results. However, the discrepancies were all on the conservative side with capacities exceeding the predicted values. The predicted values, the tested values and the percent differences are shown in table 5-3.

Table 5-3: Predicted Values, Tested values, and percent differences

Girder designation	Tested Max Load (kips)	Predicted Max Load (kips)	% increase or decrease compared to prediction
PS-1	75.87	81.9	Decrease 7.3%
PS-2	61.88	66.5	Decrease 6.9%
PS-3	90.14	79.7	Increased 13%
PS-4	84.75	79.7	Increased 6.3%
PS-5	78.92	79.7	Decreased 0.9%
PS-6	100.91	85.6	Increased 17.8%
PS-7	104.42	85.6	Increased 21.9%
PS-8	99.16	85.6	Increased15.8%
PS-9	77.26	79.7	Decreased 3.1%
PS-10	87.68	79.7	Increased 10.0%

5.2 METHOD OF ANALYSIS

5.2.1 Capacity Prediction Model: ACI440.2 R-08

Similar to designing any structural member the nominal moment multiplied by the Phi value must be greater than the ultimate moment of the beam as seen in equation 1.

$$\varphi M_n \geq M_u \tag{1}$$

This method uses the theoretical strain at the level of the CFRP; equation 2 is used to calculate the theoretical strain developed at the soffit to initiate debonding.

$$\varepsilon_{fd} = 0.083\sqrt{\frac{f_c}{nE_f t_f}} \leq 0.9\varepsilon_{fu} \tag{2}$$

The value calculated for the designed test beams for both the first RC set and the second RC set are .0098 in/in and .0069 in/in respectfully.

The effective strain level in the CFRP reinforcement at the ultimate limit state can be found from equation 3.

$$\varepsilon_{fe} = \varepsilon_{cu}\left(\frac{d_f - c}{c}\right) - \varepsilon_{bi} < \varepsilon_{fd} \tag{3}$$

Where ε_{bi} is the initial strains and should be excluded from the strains in the FRP system. Unless all loads on the member, including the self-weight are removed before installation, initial strains will exist. In the case of this research the CFRP was applied on fully supported inverted beams, thus initial strains are assumed to be zero. The calculated value for the test specimens are .016 in/in for the first RC set and .012 in/in for the second RC set; therefore ε_{fd} controls failure.

$$f_{fe} = E_f \varepsilon_{fe} \tag{4}$$

Equation 4 provides the effective maximum stress level in the CFRP that can be developed before flexural failure of the section; assuming perfectly elastic behavior. The value for the material used is calculated to be 136.9ksi.

Then, based on the strain level in the CFRP reinforcements, the strain level in the non-prestressing steel can be found from equation 5.

$$\varepsilon_s = \left(\varepsilon_{fe} + \varepsilon_{bi}\right)\left(\frac{d-c}{d_f-c}\right) \tag{5}$$

The calculated values for each set of repaired beams are 0.008 in/in and 0.006 in/in for the first RC set and second RC set, respectfully.

The stress developed in the steel can then be determined from the strain level in the steel using its stress-strain curve as shown in equation 6.

$$f_s = E_s\varepsilon_s \leq f_y \tag{6}$$

The steel used rendered a value exceeding f_y so a value of 60ksi is used as the stress developed in the steel.

Next, with the strain and stress levels in both the CFRP and the steel for the assumed neutral axis, the internal force equilibrium may be checked using equation 7.

$$c = \frac{A_s f_s + A_f f_{fe}}{\alpha_1 f'_c \beta_1 b} \tag{7}$$

The calculated neutral axis was determined to be 1.55in (39.37mm) for the first RC set of beams and 1.99in (50.55mm) for the second RC set of test beams.

Once an accurate neutral axis is found through iterative processes the nominal moment of the beam with CFRP applied can be calculated using equation 8.

$$M_n = A_s f_s\left(d\frac{\beta_1 c}{2}\right) + \psi_f A_f f_{fe}\left(h\frac{\beta_1 c}{2}\right) \tag{8}$$

The nominal moment calculated for the two sets of test beams are 26.51kip-ft for the first RC set and 33.06kip-ft for the second RC set.

The remaining two equations are related to predicting stresses in both the steel reinforcements and the CFRP reinforcements at service loads. Equation 9 provides

calculations for the stresses in the steel and equation 10 for the calculations of stresses in the CFRP.

$$f_{s,s} = \frac{\left[M_s+\varepsilon_{bi}A_fE_f\left(d_f-\frac{kd}{3}\right)\right](d-kd)E_s}{A_sE_s\left(d-\frac{kd}{3}\right)(d-kd)+A_fE_f\left(d_f-\frac{kd}{3}\right)(d_f-kd)} \quad (9)$$

$$f_{f,s} = f_{s,s}\left(\frac{E_f}{E_s}\right)\frac{d_f-kd}{d-kd} - \varepsilon_{bi}E_f \quad (10)$$

The calculated values for these two equations can be evaluated at various loads and are used to determine the behaviors of the beams as it relates to their respectful failure modes. Further discussion of the stresses and strains developed in both the steel and the CFRP are presented in following sections.

From this capacity prediction model a comparison of the theoretical values and the tested values can be completed. From evaluating the comparisons, the configurations that appear to best fit the design model are 2-14 and 2-19. Though many may be similar, the assumptions listed by the design model document must be considered.

5.2.2 **Deflection Prediction Model:** Charkas et al. 2003

To reemphasis, this prediction model is used because the ACI 440.2R-02 does not provide deflection provisions specific for FRP-strengthened beams but rather refers the designer to ACI 318-99. Furthermore, the ACI 318-99 does not address post-yielding deflections for strengthened beams (El-Mihilmy and Tedesco 2000). The assumptions that this model makes, include:

1. Concrete in compression is assumed to behave linearly up to an extreme fiber stress of 0.7 (f'_c), after which Hognestad's parabolic equation is used.

2. The equivalent rectangular stress block is used to replace the parabolic stress distribution at any stage of nonlinear analysis.
3. Reinforcing steel is assumed to have the classical linear elastic-perfectly plastic response.
4. Unidirectional FRP laminates are used. These are known to behave linearly up to failure.
5. The section moment of inertia before cracking is that of the transformed gross value (I_g).
6. The section moment of inertia is assumed to reduce to the fully cracked value (I_{cr}) upon steel yielding, if the concrete response in compression is still linear. If not, the section effective moment of inertia (I_{es}) reduces further and it is calculated from nonlinear analysis. This assumption is confirmed to be accurate by comparisons with experimental results
7. The effective section moment of inertia at ultimate level is determined by $I_n = M_n / E_c \mathrm{f}_n$
8. The section moment-curvature response is assumed to be trilinear. This model considers some tension stiffening effects because the effective section rigidity $E_c I_g$ after cracking is gradually reduced from $E_c I_g$ to $E_c I_y$, $I_y = M_y / E_c \mathrm{f}_y$ (or $E_c I_{cr}$ when linear analysis is applicable);
9. The curvature distribution along the beam span is obtained from the moment diagram and the moment-curvature relationship.
10. The external FRP plate is assumed to extend along the entire clear span and to be cut off just before the supports, when developing the closed form solutions. The

small, unstrengthened region close to the supports is expected to add a negligible extra deflection.

11. The FRP plate is assumed perfectly bonded to the beam, which is expected to be accurate especially with proper transverse anchorages.
12. The load-deflection response is determined herein up to the ultimate flexural strength. One can use strength equations developed by others to predict premature failure loads and then utilize the present load-deflection curve up to these premature failure load levels.

The major equations included in the model relevant to the this research and the corresponding calculated values for the designed test beams are presented as follows at various selected loads. Some of the listed equations are specific to four-point loading schemes; for full documentation refer to Charkas et al. 2003

Precracking stage: The first stage yields the classical uncracked (prismatic) beam problem with mid-span deflection calculated from equation 11 where ϕ_a is calculated using equation 12.

$$\Delta_{midspan} = \frac{\phi_a}{24}(3L^2 - 4{L_a}^2 \quad (11)$$

$$\phi_a = \frac{PL_a}{2E_cI_g} \quad (12)$$

The level chosen for evaluation of this stage was the cracking load; which was a value of 3.43kip (15.26N) for both the first RC set and second RC set. This load value rendered deflection and curvature values of 0.042in (1.01mm) and $5.2E^{-5}$rad for both the first set and the second set.

Postcracking stage: In this stage of loading (L_g), identifies the extent of the uncracked region where $M_{cr} = f_r I_g/c_t$; f_r = the modulus of rupture according to ACI 318-99; and c_t = distance between the neutral axis of the uncracked transformed section to the extreme fiber in tension.

$$L_g = \frac{2M_{cr}}{P} \tag{13}$$

The moment-area theorem is used to obtain the mid-span deflection by analytical integration of the moment of curvature distribution along half the span about the hinge support where f*a* is calculated by linear interpolation between the cracking curvature f_{cr} and the yielding curvature f_y.

$$\Delta_{midspan} = \frac{\phi_a}{24}\left(3L^2 - 4{L_a}^2\right) + \frac{(L_g + L_a)}{6}(\phi_{cr}L_a - \phi_a L_g) \tag{14}$$

$$\phi_a = \frac{(\phi_y - \phi_{cr})(M_a - M_{cr})}{(M_y - M_{cr})} + \phi_{cr}M_a = \frac{PL_a}{2} \tag{15}$$

The load chosen for evaluation of this stage was 18.18kip (80.87N) for the first RC set and 22.67kip (100.84N) for the second set. These load values rendered deflection and curvature values of 0.675in (17.15mm) and $8.7E^{-4}$rad for the first set and values of .846in (21.49mm) and $1.1E^{-3}$rad for the second set.

Postyielding stage: Upon yielding of the tensile steel, sections in the post-yielding stage are assumed to be fully cracked. This assumption is verified to be very accurate because the effective (I_e) of the section beyond yielding, from nonlinear analysis considering tension stiffening, is comparable to or less than that of (I_{cr}). The mid-span deflection at any load level after yielding is analytically formulated by determining the moment of the area under curvature distribution. (L_y) is the length of the unyielded regions of the beam from the support as described in equation 16.

$$L_y = \frac{2M_y}{P} \tag{16}$$

The deflection at mid-span can then be calculated by using equation 17 where the value of ϕ_a can be calculated using equation 18.

$$\Delta_{midspan} = \frac{\phi_a}{24}\left(3L^2 - 4{L_a}^2\right) + \frac{L_y}{6}\left[\phi_{cr}\left(L_y + L_g\right) - \phi_a\left(L_y + L_a\right)\right] + \frac{\phi_y\left(L_a - L_g\right)\left(L_a + L_y + L_g\right)}{6} \tag{17}$$

$$\phi_a = \frac{\left(M_a - M_y\right)\left(\phi_a - \phi_y\right)}{\left(M_a - M_y\right)} + \phi_y \tag{18}$$

The value calculated of (L_y) for each set of designed test beams is approximately 3in for both of the RC sets. However, only the deflection and curvature values were calculated and reported as 1.37in (34.8mm) and 0.0017rad for the second set of RC beams.

5.3 PRESENTATION OF RESULTS

All numerical are available in previous tables 5-1 through 5-3. However, figure 5-1 displays a graphical comparison of the theoretical load-deflection values, at cracking and ultimate stages, calculated from the two models presented and the tested values of an associated repair design configuration. Since the models do not consider the inclusion of intermediate U-wrappings the beam chosen does not utilize any either (RC 2-19).

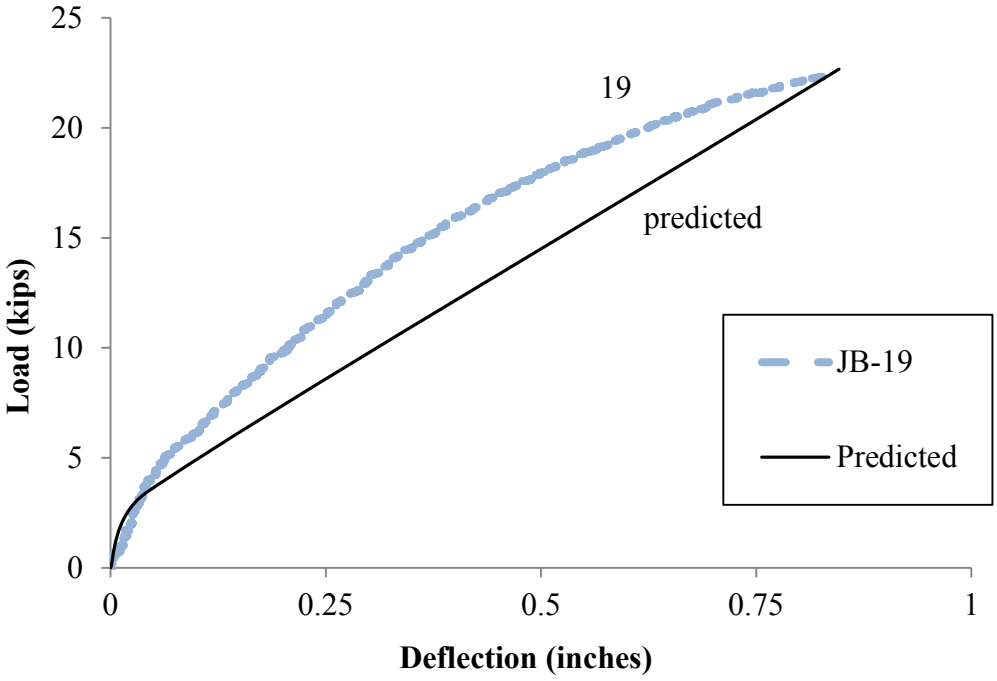

Figure 5-1: Predicted load vs. deflection for second RC set

CHAPTER 6:
DISCUSSIONS AND CONCLUSIONS

6.1 DISCUSSION OF RESULTS

From the results of the RC beam sets, CFRP repairs resulted in a wide range of flexural capacity increases from 22% to 353% compared to control damaged beams, depending on the reinforcement ratio, CFRP layers, and U-wrapping configuration. The load capacity increase varied depending on the reinforcement ratio and level of damage. In one beam set, the increase was from 52% to 92% compared to that of control damaged beam. In the other beam set, it was 101% to 353% compared to that of control damaged beam.

The CFRP repair of damaged beams (RC 1-3 to RC 1-15) not only restored the lost 27.7% of flexural capacity for undamaged beam (RC 1-1) due to the impact damage, but also enhanced the beams' capacities to exceed the original capacity of intact undamaged control beam (RC 1-2) by a range of 10% to 39%. Also, the CFRP repair of damaged beams (RC 2-3 to RC 2-19) not only restored the lost 23% of beams' carrying capacity due to the impact damage but also enhanced their capacities to exceed the capacity of intact undamaged control beam (RC 2-1) by a range of 54% to 193%.

This study agrees with the ACI 440.2R-08 document and claims that the existing prediction model provides adequate to conservative capacity estimations for repair designs, provided that the transverse CFRP U-wrappings are used appropriately to mitigate early debonding failures.

The test results indicated that the repairs greatly decrease the soffit's max tensile strain felt by the member at mid-span when compared to the control beams. Also, when comparing the repairs with intermediate anchors (RC 2-11 & RC 2-12) to one without intermediate anchors (RC 2-19) the reduction is evident. Yet, what is interesting is that the repair which utilizes spacing experiences similar to the fully wrapped beam.

From the reported results, it can be seen that although the fully wrapped beam reduces the strain more throughout the length of the beam, the configuration with spaces between anchoring appears to similarly reduce the strain at the mid-span (the critical location of damaged steel reinforcements) at higher loads.

It can also be seen from the results that the use of intermediate U-wrappings for anchoring does suppress the strain developed in the longitudinal laminate applied to the beams soffit. Intermediate anchoring u-wrappings can help to mitigate debonding by suppressing the strain felt by the longitudinal CFRP laminate.

Similarly, the results of the testing indicate that the longitudinal CFRP reinforcement should extend as far as possible within the span and defiantly should terminate no closer than specified in the ACI 440.2R-08 for development length requirements.

6.2 FACTORS AFFECTING RESULTS

The factors affecting the results of the testing are limited. Through the analysis of the measured strains it became evident that the applied strain gages on the surface of the concrete members tested broke at early load values due to the cracking of the concrete sections. This is evident for a load of 7.5 kips in RC 2-1 and loads of 5 kips and higher for the damaged control RC 2-2. It would have been more desirable to have internal

strain gages implemented inside of the concrete beams attached to the steel reinforcements.

6.3 VALIDITY OF HYPOTHESIS

As previously mentioned, it was believed that through the efforts of conducting an extensive experimental program of testing real structural components with simulated lateral damage and various CFRP repairs, an accurate and justified design procedure could be developed to assist the state transportation department in designing cost effective CFRP repairs for future incidents of overheight vehicle collisions. Through the efforts of analyzing the recorded results from testing approximately 40 beams an updated design procedure has been presented and the hypothesis has been determined to be valid.

6.4 CONCLUSIONS FROM THE STUDY

6.4.1 RC Beam Conclusions

1. The use of CFRP laminates in repair of laterally damaged beams and increases load carrying capacity for the beams while reducing deflection.
2. The repaired beams with CFRP longitudinal strip without transverse U-wraps result in premature CFRP debonding.
3. A significant increase of load carrying capacity of about…% can be achieved by using the CFRP longitudinal soffit laminates combined with U-wrappings.
4. The ACI 440.2R-08 document provides adequate to conservative capacity estimations for repair designs, provided that transverse U-wrappings are used appropriately to mitigate early debonding failures.

5. The use of CFRP laminates with different lengths at the soft indicated that the longitudinal CFRP reinforcement should extend as far as possible within the span and should terminate no closer than specified in the ACI 440.2R-08 for development length requirements.
6. In case the CFRP shear enhancements are not needed, the configuration of transverse U-wraps with spacings between them has shown to provide the same flexural benefits when compared to a fully wrapped beam.
7. Evenly spaced transverse U-wrappings provide the most efficient configuration for CFRP flexural enhancement repairs to mitigate debonding.
8. Without consideration for shear enhancements, the optimum spacing for transverse anchoring is theorized to be between a distance of $^2/_3d$ and $2d$, where d is the height of the girder (or ½ to 1½ the height of the entire composite cross-section). Yet, the recommendation is to keep the spacing between the transverse U-wrapping to $d/2$ to $2/3d$.
9. When repairing laterally damaged girders having a loss of steel reinforcements, it is necessary to cover the damaged section with transverse and longitudinal strips to reduce the crack propagation in the critical region which initiates early debonding.

6.4.2 PSC Girder Conclusions

1. The longitudinal CFRP strips applied to the girder soffit along with U-wrapping instead of full wrap proved to be an excellent repair alternative for damaged girders.

2. The use of CFRP laminates in repair of laterally damaged girders reduces deflection and increases load carrying capacity for the girders.
3. A significant increase of girders' load carrying capacity of about…% can be achieved by using the CFRP longitudinal soffit laminates combined with U-wrappings.
4. Different U-wrapping configurations with varied spacing have proven to significantly enhance the flexural capacity of damaged prestressed concrete girders and prevent premature debonding of longitudinal laminates.
5. A comparison between the failure load of a control girder (with cut strand and un-strengthened with CFRP) and repaired girders with 2 layers of CFRP shows that CFRP repair enhanced the flexural capacity by 27.53% to 45.66%.
6. For repaired girders with 3 layers of CFRP, increases in the flexural capacity were reported to range from 60.24% to 68.74% when compared to control girder (with cut strand and un-strengthened with CFRP).
7. An increase in the failure load of 24.85% to 41.69% was observed for the fully CFRP wrapped repaired girders compared to the un-strengthened control girder.
8. Proper CFRP repair design in terms of the number of CFRP longitudinal layers and U-wrapping spacing could result in obtaining significant enhancement for the capacity and desired failure modes for the repaired girders.
9. Favorable failure modes of the repaired girders can be maintained using a CFRP repair configuration utilizing spacing between the U-wrappings to prevent undesirable modes of failure such as debonding of the longitudinal CFRP strips from the girder concrete soffit. If shear improvement are not needed, spacing

close to that of the depth of the composite girder can be applied for the U-wrap configuration design to constitute a safe CFRP repair.

10. The optimum spacing for transverse anchoring is determined to be between a distance of ½ d and $^{2}/_{3}d$, where *d* is the height of the girder.
11. Debonding of some U-wraps was experienced at high loading levels after restoring the girders' virgin flexural capacity. Therefore, it is recommended that another CFRP strip be applied in the longitudinal direction at the top of the girder web to anchor the top end of the U-wraps. That will mitigate premature failure of girders
12. The repaired CFRP girders experienced a more brittle failure than control undamaged beams having no CFRP. That requires caution in the design.

6.5 RECOMMENDATIONS DERIVED FROM STUDY

The following sets of recommendations are derived from the procedures and considerations provided by the ACI 440.2R-08 and have been confirmed, altered, or enhanced based on the included research or the previously confirmed research conducted by others. These following recommendations are provided specifically for the repair of laterally damaged concrete bridge girders repaired with non-prestressed uni-directional CFRP fabric.

6.5.1 CFRP Repair Design Calculations

1. The first action to be taken is to evaluate the structural member affected by the lateral damage. The evaluation should document the existing dimensions of the structural members; the location, and size of cracks and spalls; the location and extent of any corrosion of reinforcing steel; the presence of any active corrosion;

the quality and location of existing reinforcing steel; the in-place compressive strength of the concrete; and the soundness of the concrete, particularly the concrete cover in all areas where the FRP system is going to be bonded to the concrete.

2. Next, use the information which was gathered from the evaluation in step 1 and verify that a non-prestressed CFRP repair system is applicable to the level of damage sustained. Where the damage levels may include *Minor Damage, Moderate Damage, Severe Damage*, or *Severe I*; provided that the loss of prestressing force is less than 25% where the levels of damage are defined as:

   Minor Damage: defined as; concrete with shallow spalls, nicks and cracks, scraps and some efflorescence, rust or water stains. Damage at this level does not affect a member's capacity. Repairs are for aesthetic or preventative purposes.

   Moderate Damage: will include; larger cracks and sufficient spalling or loss of concrete to expose strands. Moderate damage does not affect a member's capacity. Repairs are intended to prevent further deterioration.

   Severe Damage: is classified as; any damage requiring structural repairs. Typical damage at this level includes significant cracking and spalling, corrosion and exposed and broken strands.

Severe I: the experienced damage requires structural repair that can be affected using a non-prestressed or post-tensioned method. This may be considered as repair to affect the strength (or ultimate) limit state.

3. If a non-prestressed repair system is applicable from step 2, check that the damaged member's existing strength is sufficient to resist a level of load described by ACI440.2R-08 equation 9-1 or if the structure requires a fire rating it must satisfy ACI440.2R-08 equation 9-2.

$$(\phi R_n)_{existing} \geq (1.1S_{DL} + 0.75S_{LL})_{new} \qquad \text{(ACI Eq. 9-1)}$$

Where $(\phi R_n)_{existing}$ is the existing strength of the damaged structural member. Similarly, S_{DL} and S_{LL} are the dead and live loads expected on the repaired structural member.

$$R_n \geq S_{DL} + S_{LL} \qquad \text{(ACI Eq. 9-2)}$$

Where Rn is the nominal resistance of a member at an elevated temperature as determined in ACI 216R and the loads are as previously defined.

4. If appropriate equation in step 3 is satisfied open affiliated excel spreadsheet and enter dimensional values and material properties in the yellow cells of the input tab. A display of the input tab is shown below in figure 6-1

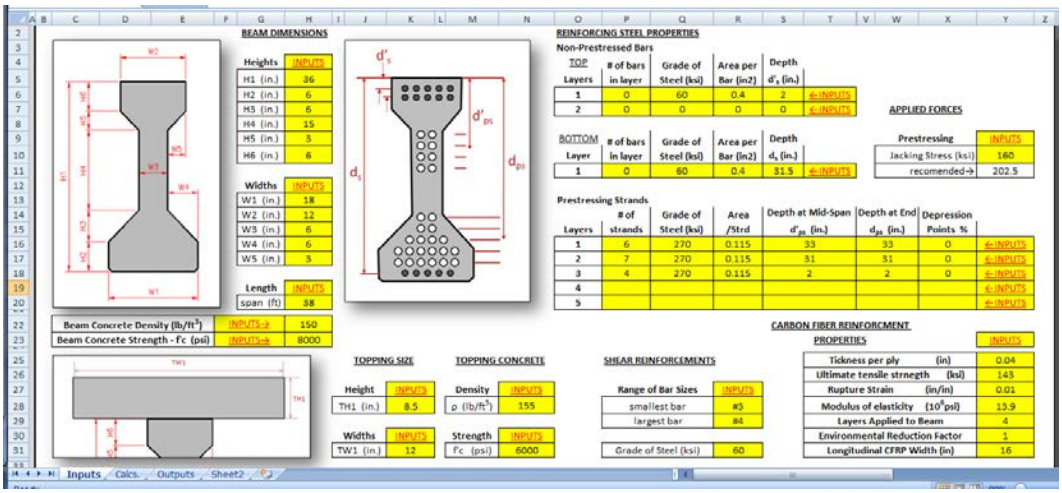

Figure 6-1: Display of input tab from affiliated excel spreadsheet

5. After entering all values required for input tab check the output tab and verify that the calculated ultimate moment is at least equivalent to that of the girder of interest prior to damage. If calculated ultimate moment is not sufficient return to input page and increase the width or number of layers of the CFRP, if ultimate moment exceeds that of the undamaged girder in question return to input page and decrease the same values. Repeat until most desirable width and number of layers is selected. Figure 6-2 shows output tab of excel spreadsheet.

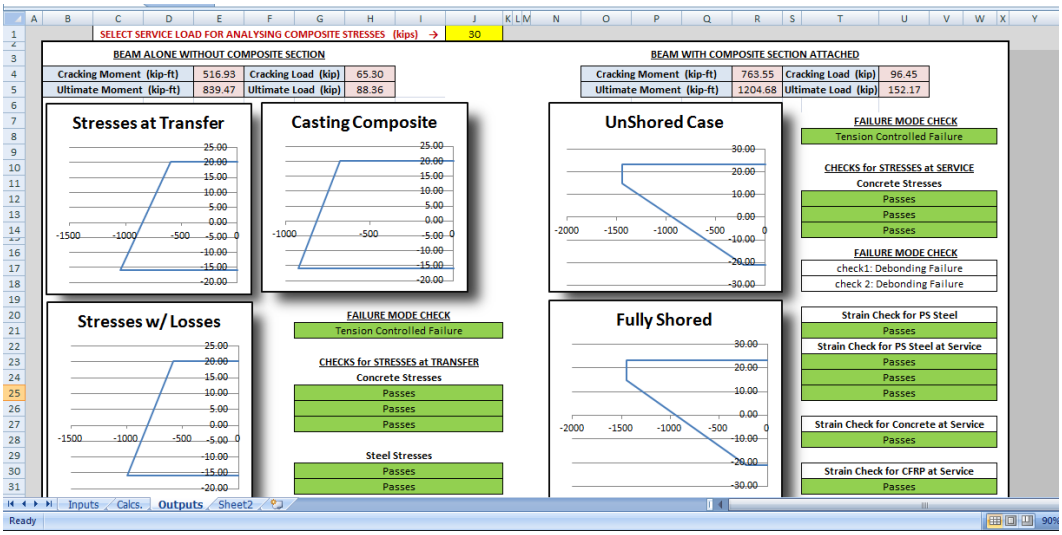

Figure 6-2: Display of output tab from affiliated excel spreadsheet

6. After the desired level of strengthening is established with the use of the provided excel spreadsheet determine the maximum spacings of the transverse U-wrapping by multiplying the height of the girder plus the composite deck by 2/3 if capacity enhancements are not required.
7. If the desire of the repair is also to provide strength enhancements for expected increased loading, follow the calculations and procedures listed in chapter 12 of the ACI440.2R-08 for shear design to establish the maximum spacings of the transverse U-wrappings using the enhanced properties of the structural member. (the smaller value of step 6 and 7 should be used if step 7 is applicable)
8. Determine the minimum length between transverse U-wrappings by computing the critical length related to the bond capacity in ACI equation 13-2.

$$l_{df} = 0.057\sqrt{\frac{nE_f t_f}{\sqrt{f'c}}} \qquad \text{(ACI Eq. 13-2)}$$

$$l_{df} = \sqrt{\frac{nE_f t_f}{\sqrt{f'c}}} \qquad \text{(ACI Eq. 13-2)}$$

Where l_{df} is the critical length, n is the number of layers, E_f is the modulus of elasticity of the CFRP, t_f is the thickness of the fibers, and $f'c$ is the compressive strength of the concrete girder.

9. If step 7 was applicable and the maximum spacings are less than the width of the CFRP U-wrappings or the value calculated in step 8 a fully wrapped arrangements of the transverse layers is recommended.

6.5.2 Implementing the Calculated Design Values

1. Provide the first longitudinal layer extending the entire span of the damaged girder's soffit and each subsequent layer provided should be one foot shorter than

the previous until the desired amount of layers determined in step 5 of section 7.2.1 is reached.

2. Provide longitudinal layers on the bottom flange of the girder approximately equal to 60% of the beams span centered over the damaged area. If the number of layers used on the girder's soffit is greater than 1 then 2 layers shall be used on the bottom flanges otherwise only 1 is required. Additional layers should be one foot shorter than the previous as in step 1.
3. Provide one longitudinal layer on the web of the girder over the damaged area. This layer could be as short as a few feet but must be greater than length calculated in step 8 of section 7.2.1. The intention is to cover any area affected by the damage to prevent crack propagations in the critical region.
4. Provide overlapping transverse U-wrappings covering the damaged area of the girder and provide spaced U-wrappings between the damaged area and the supported ends of the girder. The spacings should be adjusted between the minimum and maximum lengths determined in 7.2.1 so that each longitudinal layer terminates underneath one of the transverse U-wrappings. The amount of layers provided for each transverse section should equal the amount of soffit longitudinal layers minus 2, but must be greater than or equal to 1. The additional layers of U-wrapping do not change sizes and they should extend at least up to the top of the web.

6.5.3 Applying the CFRP Repair

1. Surface Preparation: In general, the surface must be clean, dry and free of protrusions or cavities, which may cause voids behind the composite.

Discontinuous wrapping schematics typically require a light sandblasting, grinding or other approved methods to prepare for bonding. Sharp corners should be ground down to a radius of approximately .5 inches.

2. Mixing: Pour the contents of component B into the pail of component A. Mix thoroughly for five minutes with a low speed mixer at 400-600 RPM until uniformly blended. If material is too thick, heat unmixed components by placing containers in hot tap water or sunlight until desired viscosity is achieved. The epoxy may also be thickened in the field to the desired consistency by adding fumed silica.
3. Application: Apply epoxy to surface as a primer coat. Then, uniformly saturate the fabric by hand and apply to the surface. Next, using a roller or a trowel, press the fabric to surface and work out any air voids or pockets of thick epoxy.
4. Quality Control: If voids behind the cured CFRP laminates are present, use the same epoxy and inject it into voids using traditional injection methods.
5. If a more detailed application procedure is required it is recommended to refer to section 3.3 of this document, instructions provided by the manufacturer of the product being used, or the information in theACI440.2R-08.

REFERENCES

1. ACI Committee 440, "ACI 440.2R-08 Guide for the Design and Construction of Externally Bonded FRP Systems for Strengthening Concrete Structures", American Concrete Institute, Farmington Hills, MI., 2008, pp. 80.
2. Agrawal, A.K. and Chen, C., "Bridge Vehicle Impact Assessment", Project #C-07-10, New York State Department of Transportation, 2008.
3. Brena, Sergio F., Wood, Sharon L., and Kreger, Michael E., 2003, Full-Scale Tests of Bridge Components Strengthened Using Carbon Fiber-Reinforcing Polymer Composites, ACI Structural Journal, V. 100, No. 6, November-December, American Concrete Institute.
4. Di Ludovico, M., "Experimental Behavior of Prestressed Concrete Beams Strengthened with FRP", Report CIES 03-42, University of Missouri-Rolla, MO., 2003.
5. ElSafty, A., and Graeff, M., "Investigating the Most Effective CFRP Configuration in Repairing Damaged Concrete Beams due to Collision", The 13th Internat5ional Conference on Civil, Structural and Environmental Engineering Computing, Crete, Greece, CC2011/2011.
6. El-Tawil, S. and Okeil, A. M., "LRFD Flexural Provisions for PSC Bridge Girders Strengthened with CFRP Laminates", Vol. 99, No. 2, March-April, pp. 300-310
7. Fu, C.C., Burhouse, J.R. and Chang, G. L., "Study of Overheight Vehicles with Highway Bridges", Transportation Research Board, 2003.
8. Grace, N. F., Ragheb, W. F. and Abdel-Sayed, G., "Flexural and Shear Strengthening of Concrete Girders Using New Triaxially Braided Ductile Fabric", ACI Structural Journal, V. 100, No. 6, November-December 2003.
9. Green, P. S., Boyd, A. J., and Lammert, K., "CFRP Repair of Impact-Damaged Bridge Girders, Volume I: Structural Evaluation of Impact Damaged Prestressed Concrete I Girders Repaired with FRP Materials", BC-354 RPWO #55, Florida Department of Transportation, 2004.
10. Harries, K.A., "Structural Testing of Prestressed Concrete Girders from the Lake View Drive Bridge, ASCE Journal of Bridge Engineering, V. 14, No. 2, pp. 78-92.
11. Kasan, J. L., "Structural Repair of Prestressed Concrete Bridge Girders", MSCE Thesis, University of Pittsburgh, Pennsylvania, 2009.
12. Kasan, J.L. and Harries, K. A., "Repair of Impact-Damaged Prestressed Concrete Bridge Girders with Carbon Fiber Reinforced Polymers", Asia-Pacific Conference on FRP in Structures, Seoul, Korea, December 2009.
13. Klaiber, W. F., Wipf, T. J. and Kempers, B. J., "Repair of Damaged Prestressed Concrete Bridges Using CFRP", Mid-Continent Transportation Research Symposium, Iowa State University, 2003

14. Nanni, A., Huang, P.C. and Tumialan, J.G., "Strengthening of Impact-Damaged Bridge Girder Using FRP Laminates", 9th Int. Conf., Structural Faults and Repair, London, UK., Engineering Technics Press, July, 2001.
15. Nanni, A., Huang, P.C. and Tumialan, J.G., "Strengthening of Impact-Damaged Bridge Girder Using FRP Laminates", 9th Int. Conf., Structural Faults and Repair, London, UK., July 2001, Engineering Technics Press.
16. Razaqpur, G. A. and Isgor, B., "Proposed Shear Design Method for FRP-Reinforced Concrete Members without Stirrups", ACI Structural Journal, V. 103, No. 1, January-February 2006.
17. Rosenboom, O. A., Miller, A. D., and Rizkalla, S., "Repair of Impact-Damaged Prestressed Concrete Bridge Girders using CFRP Materials", ACSE Journal of Bridge Engineering, accepted for publication 2011.
18. Schiebel, S., R.Parretti, and Nanni, A., "Repair and Strengthening of Impacted PC Girders on Bridge", Report A4845, Missouri Department of Transportation, 2001.
19. Shanafelt, G.O. and Horn, W.B., "Damage Evaluation and Repair Methods for Prestressed Concrete Bridge Members", NCHRP Report 226, Project No. 12-21, Transportation Research Board, Washington, D.C., 1980.
20. Shanafelt, G.O. and Horn, W.B., "Guidelines for Evaluation and Repair of Prestressed Concrete Bridge Members", NCHRP Report 280, Project No. 12-21(1), Transportation Research Board, Washington, D.C., 1985.
21. Shin, Y. and Lee, C., "Flexural Behavior of Reinforced Concrete Girders Strengthened with Carbon Fiber-Reinforced Polymer Laminates at Different Levels of Sustaining Load", ACI Structural Journal, V. 100, No.2, March-April 2003.
22. Stallings, J.M., Tedesco, J.W., El-Mihilmy, M., and McCauley, M., "Field Performance of FRP Bridge Repairs", Journal of Bridge Engineering, V. 05, No.5, 2000, pp. 107-113.
23. Tumialan, J.G., Huang, P.C, and Nanni, A., "Strengthening of an Impacted PC Girder on Bridge A10062", Final Report RDT01-013/RI99-041, Missouri Department of Transportation, 2001.